Suwabe N, Takahashi S, Nakano T, Yamamoto M. 1998. GATA-1 regulates growth and differentiation of definitive erythroid lineage cells during in vitro ES cell differentiation. Blood 92:4108–4118.

Takahashi K, Tanabe K, Ohnuki M, Narita M, Ichisaka T, Tomoda K, Yamanaka S. 2007. Induction of pluripotent stem cells from adult human fibroblasts by defined factors. Cell 131:861–872.

Takahashi K, Yamanaka S. 2006. Induction of pluripotent stem cells from mouse embryonic and adult fibroblast cultures by defined factors. Cell 126:663–676.

Toda Y, Kono K, Abiru H, Kokuryo K, Endo M, Yaegashi H, Fukumoto M. 1999. Application of tyramide signal amplification system to immunohistochemistry: a potent method to localize antigens that are not detectable by ordinary method. Pathol Int 49:479–483.

Tulpule A, Lensch MW, Miller JD, Austin K, D'Andrea A, Schlaeger TM, Shimamura A, Daley GQ. 2010. Knockdown of Fanconi anemia genes in human embryonic stem cells reveals early developmental defects in the hematopoietic lineage. Blood 115:3453–3462.

Uchida T, Kanno T, Hosaka S. 1985. Direct measurement of phagosomal reactive oxygen by luminol-binding microspheres. J Immunol Methods 77:55–61.

Umeda K, Heike T, Yoshimoto M, Shinoda G, Shiota M, Suemori H, Luo HY, Chui DH, Torii R, Shibuya M, Nakatsuji N, Nakahata T. 2006. Identification and characterization of hemoangiogenic progenitors during cynomolgus monkey embryonic stem cell differentiation. Stem Cells 24:1348–1358.

Umeda K, Heike T, Yoshimoto M, Shiota M, Suemori H, Luo HY, Chui DH, Torii R, Shibuya M, Nakatsuji N, Nakahata T. 2004. Development of primitive and definitive hematopoiesis from nonhuman primate embryonic stem cells in vitro. Development 131:1869–1879.

van de Winkel JG, Anderson CL. 1991. Biology of human immunoglobulin G Fc receptors. J Leukoc Biol 49:511–524.

van Lochem EG, van der Velden VH, Wind HK, te Marvelde JG, Westerdaal NA, van Dongen JJ. 2004. Immunophenotypic differentiation patterns of normal hematopoiesis in human bone marrow: reference patterns for age-related changes and disease-induced shifts. Cytometry B Clin Cytom 60:1–13.

Vowells SJ, Sekhsaria S, Malech HL, Shalit M, Fleisher TA. 1995. Flow cytometric analysis of the granulocyte respiratory burst: a comparison study of fluorescent probes. J Immunol Methods 178:89–97.

Winterbourn CC. 2002. Biological reactivity and biomarkers of the neutrophil oxidant, hypochlorous acid. Toxicology 181-182:223–227.

Yokoyama Y, Suzuki T, Sakata-Yanagimoto M, Kumano K, Higashi K, Takato T, Kurokawa M, Ogawa S, Chiba S. 2009. Derivation of functional mature neutrophils from human embryonic stem cells. Blood 113:6584–6592.

Yu J, Vodyanik MA, Smuga-Otto K, Antosiewicz-Bourget J, Frane JL, Tian S, Nie J, Jonsdottir GA, Ruotti V, Stewart R, Slukvin II, Thomson JA. 2007. Induced pluripotent stem cell lines derived from human somatic cells. Science 318:1917–1920 .

OPEN ACCESS Freely available online

PLoS one

A Novel Serum-Free Monolayer Culture for Orderly Hematopoietic Differentiation of Human Pluripotent Cells via Mesodermal Progenitors

Akira Niwa[1,2], Toshio Heike[2], Katsutsugu Umeda[2,4], Koichi Oshima[1], Itaru Kato[1,2], Hiromi Sakai[5], Hirofumi Suemori[3], Tatsutoshi Nakahata[1,2], Megumu K. Saito[1,2]*

1 Clinical Application Department, Center for iPS Cell Research and Application, Kyoto University, Kyoto, Japan, **2** Department of Pediatrics, Graduate School of Medicine, Kyoto University, Kyoto, Japan, **3** Laboratory of Embryonic Stem Cell Research, Stem Cell Research Center, Institute for Frontier Medical Sciences, Kyoto University, Kyoto, Japan, **4** Institute of Molecular Medicine, University of Texas Health Science Center, Houston, Texas, United States of America, **5** Waseda Bioscience Research Institute in Helios, Singapore

Abstract

Elucidating the *in vitro* differentiation of human embryonic stem (ES) and induced pluripotent stem (iPS) cells is important for understanding both normal and pathological hematopoietic development *in vivo*. For this purpose, a robust and simple hematopoietic differentiation system that can faithfully trace *in vivo* hematopoiesis is necessary. In this study, we established a novel serum-free monolayer culture that can trace the *in vivo* hematopoietic pathway from ES/iPS cells to functional definitive blood cells via mesodermal progenitors. Stepwise tuning of exogenous cytokine cocktails induced the hematopoietic mesodermal progenitors via primitive streak cells. These progenitors were then differentiated into various cell lineages depending on the hematopoietic cytokines present. Moreover, single cell deposition assay revealed that common bipotential hemoangiogenic progenitors were induced in our culture. Our system provides a new, robust, and simple method for investigating the mechanisms of mesodermal and hematopoietic differentiation.

Citation: Niwa A, Heike T, Umeda K, Oshima K, Kato I, et al. (2011) A Novel Serum-Free Monolayer Culture for Orderly Hematopoietic Differentiation of Human Pluripotent Cells via Mesodermal Progenitors. PLoS ONE 6(7): e22261. doi:10.1371/journal.pone.0022261

Editor: Dan Kaufman, University of Minnesota, United States of America

Received January 4, 2011; **Accepted** June 18, 2011; **Published** July 27, 2011

Funding: This work was supported by grants from the Ministry of Education, Culture, Sports, Science, and Technology of Japan (#22790979). The funders had no role in study design, data collection and analysis, decision to publish, or preparation of the manuscript.

Competing Interests: The authors have declared that no competing interests exist.

* E-mail: msaito@kuhp.kyoto-u.ac.jp

Introduction

Because of pluripotency and self-renewal, human embryonic stem (ES) cells and induced pluripotent stem (iPS) cells are potential cell sources for regenerative medicine and other clinical applications, such as cell therapies, drug screening, toxicology, and investigation of disease mechanisms [1,2,3]. iPS cells are reprogrammed somatic cells with ES cell-like characteristics that are generated by introducing certain combinations of genes, proteins, or small molecules into the original cells [4,5,6,7]. Patient-derived iPS cells have facilitated individualized regenerative medicine without immunological or ethical concerns. Moreover, patient- or disease-specific iPS cells are an important resource for unraveling human hematological disorders. However, for this purpose, a robust and simple hematopoietic differentiation system that can reliably mimic in vivo hematopoiesis is necessary.

Mesodermal and hematopoietic differentiation is a dynamic event associated with changes in both the location and phenotype of cells [8,9,10,11]. Some primitive streak (PS) cells appearing just after gastrulation form the mesoderm, and a subset of mesodermal cells differentiate into hematopoietic cell lineages [9,12,13,14,15,16]. Previous studies have accumulated evidence on these embryonic developmental pathways.

The leading methods of blood cell induction from ES/iPS cells employ 2 different systems: monolayer animal-derived stromal cell coculture and 3-dimensional embryoid body (EB) formation. Both methods can produce hematopoietic cells from mesodermal progenitors, and combinations of cytokines can control, to some extent, the specific lineage commitment [1,2,17,18,19,20,21,22,23,24,25,26,27,28]. In the former method, a previous study showed that OP9 stromal cells, which are derived from the bone marrow of osteopetrotic mice, augment the survival of human ES cell-derived hematopoietic progenitors [29]. However, as the stromal cell condition controls the robustness of the system, it can be relatively unstable. Furthermore, the induction of hematopoietic cells from human pluripotent cells on murine-derived cells is less efficient than that from mice cells.

In EB-based methods, hematopoietic cells emerge from specific areas positive for endothelial markers such as CD31 [30,31,32]. Through these methods, previous studies have generated a list of landmark genes for each developmental stage, such as *T* and *KDR* genes for the PS and mesodermal cells, respectively [12,16,17,18,25,28,33,34,35,36], and also have emphasized appropriate developmental conditions consisting of specific microenvironments, signal gradients, and cytokines given in suitable combinations with appropriate timing. For robust and reproducible specification to myelomonocytic lineages of cells, some recent studies have converted to serum-independent culture by using EB formation [37]. However, the difficulty in applying 3-dimensional location information inside EBs prevents substantial increases in

hematopoietic specification efficacy. Additionally, the sphere-like structure of the EB complicates tracking and determination of hematopoietic–stromal cell interactions.

To overcome these issues, we established a novel serum-free monolayer hematopoietic cell differentiation system from human ES and iPS cells. Although there are no reports describing the shift of human ES/iPS cells from primitive to definitive erythropoiesis in a monolayer xeno-cell-free condition, our system can trace the in vitro differentiation of human ES/iPS cells into multiple lineages of definitive blood cells, such as functional erythrocytes and neutrophils. Hematopoietic cells arise via an orderly developmental pathway that includes PS cells, mesoderm, and primitive hematopoiesis.

Materials and Methods

Maintenance of human ES/iPS cells in serum-free condition

Experiments were carried out with the human ES cell lines KhES-1 and KhES-3 (kindly provided by Norio Nakatsuji) and iPS cell lines 201B7 and 253G4 (kindly provided by Shinya Yamanaka). Stable derivatives of ES cells carrying the transgene for green fluorescent protein (GFP) after CAG promoter were also used [38,39]. The ES/iPS cells were maintained on a tissue culture dish (#353004; Becton-Dickinson, Franklin Lakes, NJ) coated with growth factor-reduced Matrigel (#354230; Becton-Dickinson) in mTeSR1 serum-free medium (#05850; STEMCELL Technologies, Vancouver, BC, Canada). The medium was replaced everyday. Passage was performed according to the manufacturer's protocol.

Differentiation of ES/iPS cells

First, undifferentiated ES/iPS cell colonies were prepared at the density of less than 5 colonies per well of a 6-well tissue culture plate (#353046; Becton-Dickinson). When individual colony grew up to approximately 500 μm in diameter, mTeSR1 maintenance medium was replaced by Stemline II serum-free medium (#S0192; Sigma-Aldrich, St. Louis, MO) supplemented with Insulin-Transferrin-Selenium-X Supplement (ITS) (#51500-056; Invitrogen, Carlsbad, CA). This day was defined as day 0 of differentiation. BMP4 (#314-BP-010; R&D Systems, Minneapolis, MN) was added for first 4 days and replaced by $VEGF_{165}$ (#293-VE-050; R&D Systems) and SCF (#255-SC-050; R&D Systems) on day 4. On day 6, the cytokines were again replaced by the haematopoietic cocktail described in the result section. Concentration of each cytokine was as follows: 20 ng/mL BMP4, 40 ng/mL $VEGF_{165}$, 50 ng/mL SCF, 10 ng/mL TPO (#288-TPN-025; R&D Systems), 50 ng/mL IL3 (#203-IL-050; R&D Systems), 50 ng/mL Flt-3 ligand (#308-FK-025; R&D Systems), 50 ng/mL G-CSF (#214-CS-025; R&D Systems), 50 ng/mL complex of IL-6 and soluble IL-6 receptor (FP6) (kindly provided by Kyowa Hakko Kirin Co., Ltd., Tokyo, Japan) and 5 IU/mL EPO (#329871; EMD Biosciences, San Diego, CA). Thereafter, the medium was changed every 5 days.

Antibodies

The primary murine anti-human monoclonal antibodies used for flow cytometric (FCM) analysis are as follows: PE-conjugated anti-SSEA-4 (#330405; BioLegend, San Diego, CA), Alexa Fluor® 647-conjugated anti-TRA-1-60 (#560122; Becton-Dickinson), biotin-conjugated anti-CD140a (#323503; Biolegend), Alexa Fluor® 647-conjugated anti-KDR (#338909; BioLegend), PE-conjugated anti-CXCR4 (#555974; Becton-Dickinson), PE-conjugated anti-CD117 (#313203; BioLegend), PE-conjugated CD34 (#A07776; Beckman Coulter, Brea, CA), FITC-conjugated CD43 (#560978; Becton-Dickinson), and APC-conjugated CD45 (#IM2473; Beckman Coulter). A streptavidin-PE (#554061; Becton Dickinson) was used as secondary antibody against biotin-conjugated primary antibody. The primary antibodies used to immunostain the colonies and floating blood cells included anti-human Oct3/4 (#611203; Becton-Dickinson), T (#sc-101164; Santa Cruz Biotechnology, Santa Cruz, CA), KDR (#MAB3571; R&D Systems), VE-Cadherin (#AF938; R&D Systems), and rabbit anti-pan-human Hb (#0855129; MP Biomedicals, Solon, OH). FITC-conjugated donkey anti-rat antibodies and Cy3-conjugated goat anti-mouse antibodies (Jackson ImmunoResearch Laboratories, Inc., West Grove, PA) were used as secondary antibodies.

Cytostaining

Floating cells were centrifuged onto glass slides by using a Shandon Cytospin 4 Cytocentrifuge (Thermo, Pittsburgh, PA) and analysed by microscopy after staining with May–Giemsa or myeloperoxidase. For immunofluorescence staining, cells fixed with 4% paraformaldehyde were first permeabilized with phosphate-buffered saline containing 5% skimmed milk (Becton–Dickinson) and 0.1% Triton X-100 and then incubated with primary antibodies, followed by incubation with FITC or Cy3-conjugated secondary antibodies. Nuclei were counterstained with 4,6-diamidino-2-phenylindole (DAPI) (Sigma-Aldrich).

Flow cytometric analysis

The adherent cells were treated with Dispase (#354235; Becton-Dickinson) and harvested by gently scraping the culture dish. Aggregated cell structure was chopped by a pair of scissors, processed by GentleMACS (Milteny Biotec, Germany) and then dispersed by 40-μm strainers (#2340; Becton-Dickinson) before staining with antibodies. Dead cells were excluded by DAPI staining. Samples were analysed using a MACSQuant (Milteny Biotec) and FlowJo software (Thermo). Cell sorting was performed using a FACSVantage or FACSAria (Becton–Dickinson).

RNA extraction and real-time quantitative PCR analysis

RNA samples were prepared using silica gel membrane-based spin-columns (RNeasy Mini-KitTM; Qiagen, Valencia, CA) and subjected to reverse transcription (RT) with a Sensiscript-RT Kit (Qiagen). All procedures were performed according to the manufacturer's instructions. For real-time quantitative PCR, primers and the fluorogenic probes were designed and selected according to Roche Universal Primer library software (Roche Diagnostics) and MGB probe system (Applied Biosystems, Carlsbad, CA). The instrument used was the Applied Biosystems ABIPrism 7900HT sequence detection system, and the software for data collection and analysis was SDS2.3. A GAPDH RNA probe (Hs00266705_g1) was used to normalise the data.

Clonogenic colony-forming assay

At the indicated days of culture, from days 6 through 25, the adherent cells were treated with dispase and harvested. They were incubated in a new tissue-culture dish (#3003, Becton–Dickinson) for 10 min to eliminate adherent non-haematopoietic cells [40]. Floating cells were collected and dispersed by 40-μm strainers. After dead cells were eliminated by labeling with Dead-Cert Nanoparticles (#DC-001, ImmunoSolv, Edinburgh, UK), live hematopoietic cells were cultured at a concentration of 1×10^3 (for counting CFU-G) or 10^4 (for counting CFU-Mix, BFU-E, and CFU-GM) cells/ml in 35-mm petri dishes (#1008; Becton-Dickinson) using

1 ml/dish of MethoCult GF+ semisolid medium (#4435; STEMCELL Technologies) as previously described. Colonies were counted after 14–21 days of incubation, and colony types were determined according to the criteria described previously [41,42,43] by in situ observation using an inverted microscope. The abbreviations used for the clonogenic progenitor cells are as follows: CFU-Mix, mixed colony-forming units; BFU-E, erythroid burst-forming units; CFU-GM, granulocyte–macrophage colony-forming units; and CFU-G, granulocyte colony-forming units.

Single-cell deposition assay

The single-cell deposition assay was performed as described previously [17,18,28]. In brief, single sorted cells were deposited in individual wells of 96-well plates with confluent OP9 layers and cultured for 14 days. Wells were scored by morphological observation for hematopoietic colony detection and stained with anti-vascular endothelial cadherin (VE-cadherin) antibodies for endothelial lineage detection.

Chemotaxis assay

Chemotaxis assay was performed with modified Boyden chamber method using 3.0-μm pore size cell culture inserts (Becton Dickinson). In brief, 5×10^4 cells harvested from floating cell fraction at day 25 were added to the upper chamber and induced to migrate towards the lower chamber containing 10 nM formyl-Met-Leu-Phe (fMLP; Sigma-Aldrich) for 4 hours at 37°C. After incubation, the cells in the lower chamber were collected and counted using a MACSQuant flow cytometer (Miltenyi Biotec). For quantitative analysis, equivalent amount of 6-μm beads (Becton Dickinson) were added to each FCM sample, and the cell numbers were determined by measuring the ratio of cells to beads.

Phagocytosis and detection of reactive oxygen species

Phagocytosis and production of reactive oxygen species were detected by chemiluminescent microspheres (luminol-binding carboxyl hydrophilic microspheres; TORAY, Tokyo, Japan) as described previously [44]. In brief, 2×10^4 floating cells were suspended in 50 μL of the reaction buffer (HBSS containing 20 mM *N*-2-hydroxyethylpiperazine-*N*-2-ethanesulfonic acid (HEPES)) per tube. To activate the system, 5 μl chemiluminescent microspheres were added, and light emission was recorded continuously using a luminometer (TD-20/20; Turner Designs, Sunnyvale, CA). During the measurement, samples were kept at 37°C. To inhibit the reaction, 1.75 μg of cytochalasin B (Sigma-Aldrich) was added to the samples.

Measurement of oxygen-binding ability

Floating blood cells derived from KhES-1 and 253G4 strains were harvested on day 32 of differentiation (with erythropoietic cytokine cocktail). Oxygen dissociation curves for hemoglobin were measured using a Hemox-Analyzer (TCS Scientific Corporation, New Hope, PA) as previously reported [45,46].

Results

Stepwise generation of functional hematopoietic cells from human ES/iPS cells in the serum-free monolayer culture without animal-derived stromal cells

To assess the differentiation activity of each human ES/iPS cell line with high reproducibility, we used a chemically defined medium in the monolayer differentiation culture and succeeded in inducing various blood cells, including erythrocytes and neutrophils (Figure 1a). To present the developmental process from human ES/iPS cells to blood cells in an orderly manner, we divided the entire process into 3 steps: (1) initial differentiation into PS cells, (2) induction of the hematopoietic mesoderm (Movie S1), and (3) commitment to the hematopoietic lineages (Movie S2).

Step 1: Induction of PS-like cells from undifferentiated human ES/iPS cells with BMP4 (days 0–4). First, we examined the efficacy of initial progression from undifferentiated pluripotent cells (KhES-1) into PS-like cells according to the expression of representative marker genes, such as *T* and *Mixl1* (Figure 1b), and the change in morphology (Figure 1c). Without cytokines, these genes were only slightly upregulated during the first 4 days. However, when 40 ng/mL BMP4 was added to the culture, the expression levels of these genes increased, which is compatible with previous reports on the importance of BMP4 in mesodermal/endodermal differentiation via PS during early embryogenesis (Figure 1b). Further, transcription levels of the undifferentiated marker *Nanog* decreased. During this period, the colonies showed substantial morphological changes at the margins, and cell density decreased and cell contact diminished (Movie S1, Figure 1c). Immunohistochemical staining assays confirmed the upregulation of T and the lateral mesodermal marker, KDR, and downregulation of Oct3/4 (Figure 1c). However, regarding ectodermal commitment, the representative marker gene *Sox1* was hardly detected on day 4 in the presence of BMP4 (Figure 1b).

To assess the role of BMP4 in this step, we analyzed the differentiation efficacy of individual ES (KhES-1 and KhES-3) and iPS (201B7 and 253G4) cell strains with various concentrations of BMP4 in the presence or absence of its inhibitor, Noggin. As shown in Figure 1d, *T* gene expression was upregulated by BMP4 dose-dependently up to 20 ng/mL and was almost completely suppressed by the BMP4 inhibitor, Noggin, in both ES and iPS cells. This suggested that BMP4 was critical at this stage. From these results, we used BMP4 at 20 ng/mL concentration in subsequent experiments.

We also assayed the expression of several cell surface protein markers in this step (Figure 1e). On day 4, undifferentiated cell markers (TRA-1-60 and SSEA4) were downregulated, whereas paraxial and lateral mesoderm cell markers (CD140a and KDR) and markers for mesodermal and hematopoietic progenitors (CXCR4 and CD117) were upregulated. The early-phase hematopoietic-committed cell markers (CD34 and CD43) were still negative at this stage. Similar results were obtained for both ES and iPS cells (data not shown), suggesting that our system initiated paraxial and lateral mesodermal differentiation from pluripotent stem cells during Step 1 [33].

Step 2: Generation of $KDR^+CD34^+CD45^-$ progenitors with VEGF and SCF (days 4–6). Our previous studies of primate ES cells demonstrated that $KDR^+CD34^+CD45^-$ mesodermal progenitors derived in a VEGF-containing culture on OP9 stromal cells included hematopoietic progenitors [17,18]. Therefore, we used this data to induce these progenitors in our culture system. Considering the partial expression of KDR and CD117 during the first step, we replaced BMP4 with 40 ng/mL $VEGF_{165}$ (ligand for KDR) and 50 ng/mL SCF (ligand for CD117) on day 4 to accelerate selective differentiation to the lateral mesoderm with hematopoietic activities (Figure 1a).

During the next 2 days, the colonies exhibited 2 distinct regions: a plateau-like central area with stratified components and a surrounding area with monolayer cells (Movie S1, Figure 1c). On day 6, the mRNA expression pattern indicated the dominance of mesodermal cells rather than endodermal or ectodermal lineages

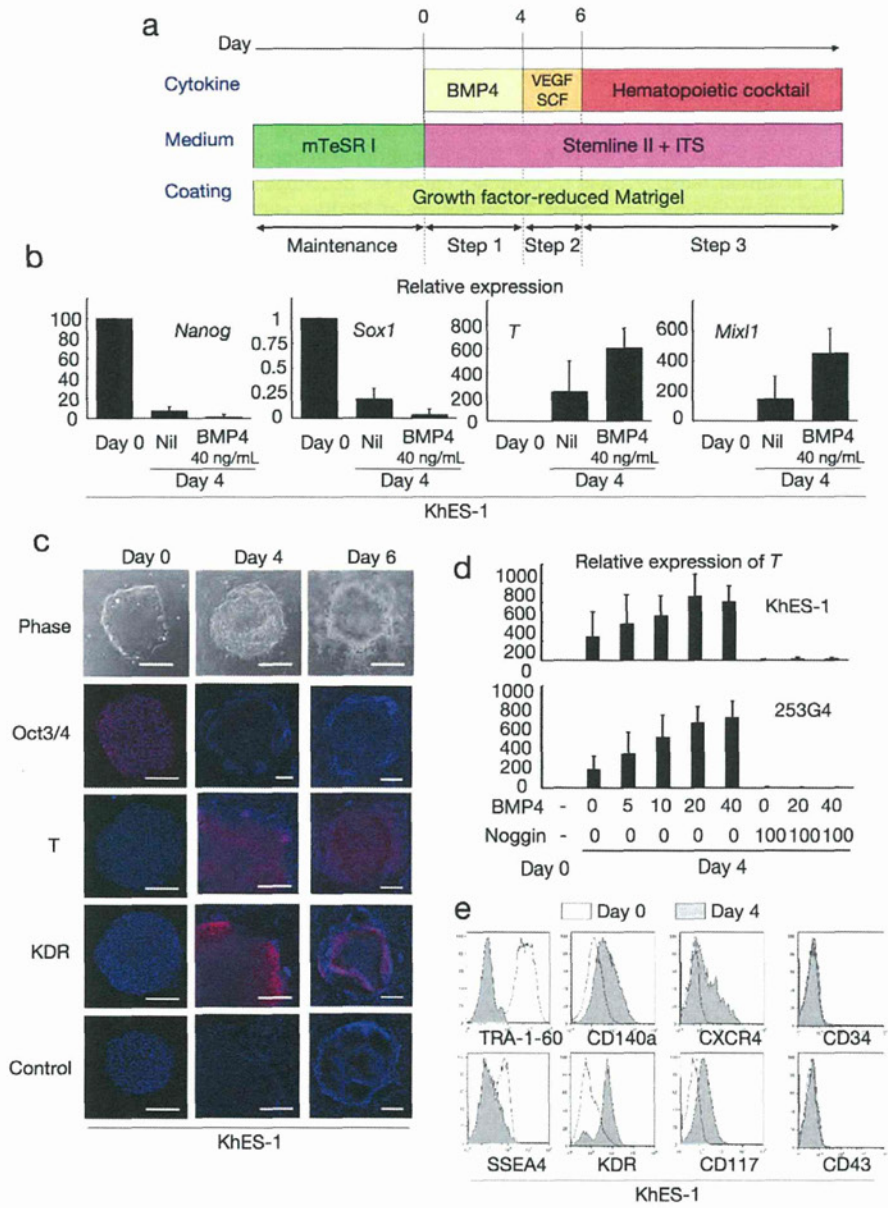

Figure 1. Blood cell induction from pluripotent stem cells starts with commitment into primitive streak. a. A schema of stepwise haematopoietic differentiation of human ES/iPS cells. **b.** Gene expression analysis of colonies at the beginning of differentiation (day 0) and the end of step 1 (day 4) with/without 40 ng/mL BMP4. Data from KhES-1 are shown as representative. **c.** Phase contrast microscopies and immunofluorescence staining of colonies during initial differentiation. Data from KhES-1 are shown as representative. **d.** Relative expression of *T* at day 4 of differentiation with different combinations of BMP4 and its inhibitor Noggin. Where shown, bars represent standard deviation of the mean of three independent experiments; Scale bars, 500 μm. Data from KhES-1 and 253G4 strains are shown as representative. **e.** Flow cytometric analysis of differentiating cells on day 4, indicating the down-regulation of immature cell markers and up-regulation of differentiated progenitor markers. Data from KhES-1 are shown as representative.
doi:10.1371/journal.pone.0022261.g001

(Figure 2a), and flow cytometric (FCM) analysis demonstrated the emergence of new cell fractions that were positive for KDR, CD117, CXCR4, and CD34 but negative for CD140a, CD43, and CD45 (Figure 2b). Our system robustly supports mesodermal induction from both ES and iPS cells, despite differences in efficacy among cell strains (Figure 2c).

Further, immunohistochemical staining for KDR indicated an uneven distribution of KDR^+ cells at the marginal zone of the plateau area (Figure 1c), suggesting that differentiation polarity within the colonies resulted in site-specific emergence of putative hematopoietic mesodermal progenitors.

Step 3: Production of functional blood cells dependent on cytokine cocktails (day 6 onward). On day 6, we changed the culture medium to another chemically defined medium containing hematopoietic cytokines (Figure 1a). To achieve lineage-directed differentiation, we used 2 combinations of cytokines: a myeloid-

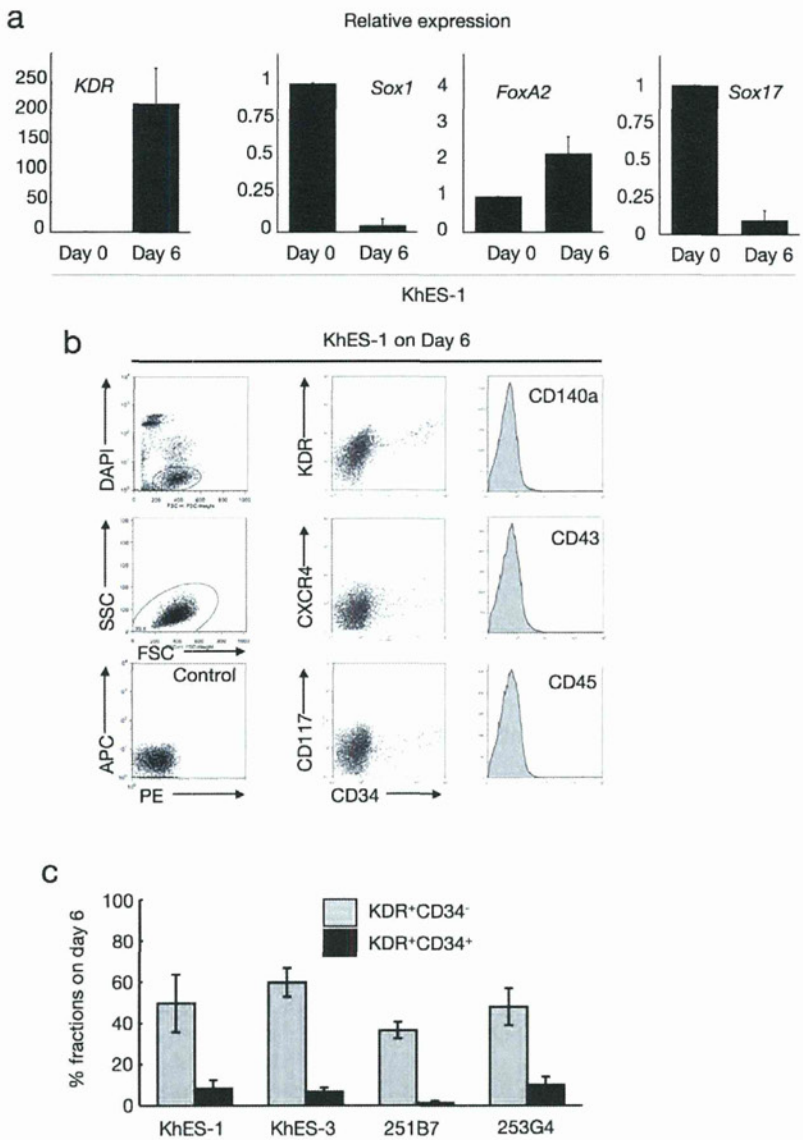

Figure 2. Characterization of cells during initial differentiation with lineage-specific marker expression. a. Expression analysis of lineage-specific marker genes at the beginning of differentiation (day 0) and the end of step 2 (day 6). Bars represent standard deviation of the mean of three independent experiments. Data from KhES-1 are shown as representative. **b.** The development of progenitors on day 6 positive for lateral mesoderm markers but negative for paraxial mesoderm and haematopoietic cell markers. Leftmost column shows the gating strategy for eliminating dead cells and debris. Data from KhES-1 are shown as representative. c. Efficacy of inducing $KDR^{+}CD34^{+\text{ or }-}$ mesodermal progenitors from each two lines of human ES cells and iPS cells. Bars represent standard deviation of the mean of three independent experiments.
doi:10.1371/journal.pone.0022261.g002

induction cocktail containing SCF, TPO, IL3, FLT-3 ligand, and G-CSF; and an erythropoietic-differentiation cocktail containing SCF, TPO, IL3, FP6, and EPO.

Regardless of the cocktails, the colonies first exhibited a rosary-like appearance, with small sac-like structures aligned along the margins of the plateau areas, and grew for several days (Figure 3a, left panel). Hematopoietic cell clusters emerged from the edge of these structures on days 10–12, followed by the appearance of floating blood cells a few days later, which increased thereafter; hematopoietic clusters grew in size and number, and some exhibited areas with a cobblestone-like appearance (Figure 3a, right 3 panels; Movie S2). When fresh medium with the cytokines was supplied every 5 days, blood cell production was observed in both ES and iPS cell experiments until day 50 of differentiation, whereas few hematopoietic cells appeared without the cytokines (data not shown).

As expected, the myeloid-induction cocktail induced myelo-monocytic lineages predominantly positive for CD45. Blood cells harvested on day 30 exhibited morphology compatible with myelomonocytic precursors and mature neutrophils, and displayed positive myeloperoxidase staining (Figure 3b). On the other hand, the erythropoietic-differentiation cocktail yielded cell lineages that included hemoglobin-positive (Hb^{+}) erythroid cells and $CD41^{+}$ megakaryocytes (Figure 3b). In the KhES-1 strain (3.5 [standard deviation (SD) = 1.5] undifferentiated colonies 250 μmm in diameter were initially plated in individual wells of 6-well plates

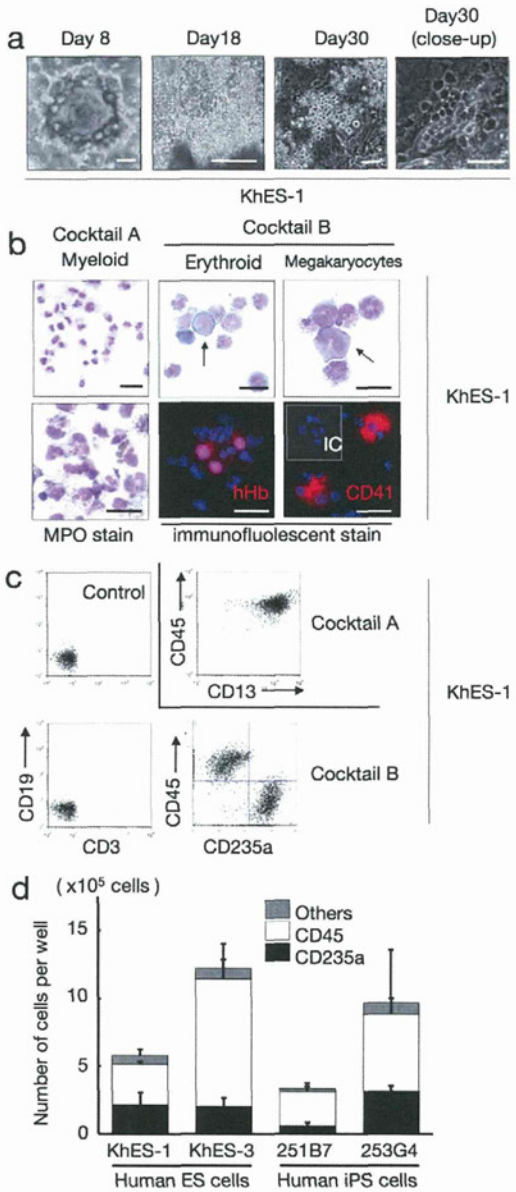

Figure 3. Human ES/iPS cell-derived haematopoiesis in a monolayer culture free from animal serum or stromal cells. a. Sequential phase contrast pictures showing haematopoietic development. Scale bars, 500 μm (left two panels) and 100 μm (right two panels). Data from KhES-1 are shown as representative. **b.** Floating cells harvested on day 30 showing various lineages of haematopoietic cells; MPO-positive myeloid lineage cells (leftmost panels), pan-human Hb-positive erythroid lineage cells (centre panels), and CD41-positive megakaryocytes (rightmost panels). Scale bars, 100 μm. Data from KhES-1 are shown as representative. **c.** Expression of lineage-specific antigens on floating cells harvested on day 30; Myeloid lineages (CD13 and CD45), erythroid lineages (CD235a), T cells (CD3), and B cells (CD19). Data from KhES-1 are shown as representative. **d.** Numbers and fraction of blood cells induced from each two lines of human ES cells and iPS cells. Bars represent standard deviation of the mean of three independent experiments.
doi:10.1371/journal.pone.0022261.g003

at the start of differentiation), counting and FCM analysis of harvested blood cells on day 30 revealed the existence of 7.7×10^5 (SD = 2.3×10^5) different cell lineages per well, including 36.0% (SD = 6.4%) CD235a$^+$ erythroid and 53.2% (SD = 9.4%) CD45$^+$ myelomonocytic lineages, but no lymphoid lineage cells (Figure 3c). Although the differentiation efficacy and lineage distribution depend not only on the cytokines but also on the cell strains, the data indicates that human ES and iPS cells develop into various lineages of hematopoietic cells, robustly and orderly, in our novel monolayer culture system without xeno-derived serum or stromal cells (Figure 3d).

ES/iPS cell-derived hematopoietic cells have similar potential to in vivo-derived blood cells in function

Considering the use of ES/iPS cell-derived hematopoiesis for various clinical and research applications, it is important to confirm the function of the generated blood cells. Neutrophils derived with the myeloid-induction cocktail exhibited migration activity in response to the chemoattractant fMLP (Figure 4a) and phagosome-dependent reactive oxygen production, which was inhibited by the phagosome destruction agent, cytochalasin B (Figure 4b). On the other hand, erythroid lineage cells derived with the erythropoietic-differentiation cocktail (harvested on day 32 of differentiation) exhibited an oxygen dissociation curve that was similar, despite being slightly left-shifted, to those obtained with adult and cord blood cells (Figure 4c). These data indicate that our culture facilitates robust and orderly development of human ES and iPS cells into functional hematopoietic cells with similar potential to in vivo-derived blood cells.

Clonogenic hematopoietic development from human ES/iPS cell-derived progenitors

The human hematopoietic system is a hierarchy of various component cells from stem or progenitor cells to terminally differentiated cells. For example, CD34$^+$ cells in umbilical cord blood or bone marrow contain putative hematopoietic stem cells and are used as a source of stem cell transplantation. The identification and proliferation of such cells in vitro have been of great interest in medical science research.

To assess the potential of our system for supporting generated immature stem or progenitor cells, we evaluated the colony-forming ability of the cultivated hematopoietic progenitors in the system. Accordingly, the cells were cultured with SCF, TPO, IL3, FLT-3 ligand, and FP6. In these conditions, CD34$^+$CD45$^+$ hematopoietic cells existed up to day 25, indicating that the immature hematopoietic cells can be maintained in our serum-free culture (Figure 5a).

We harvested adherent blood cells from the previously described culture and transferred them into a methylcellulose-containing medium to perform colony-forming assays with SCF, TPO, IL3, G-CSF, and EPO. As shown in Figure 5b and c, CFU-Mix, BFU-E, CFU-GM, and CFU-G colonies developed from plated cells. The total number of colonies increased dramatically from day 6 to day 10, then gradually increased until day 15 and decreased thereafter. CFU-Mix and BFU-E colonies were mainly observed until day 15 and were thereafter replaced by CFU-GM and CFU-G colonies. Similar tendencies were observed in both ES and iPS cells. These results suggest that our culture system can incubate multipotent hematopoietic stem or progenitor cells over a period of time.

Identification of KDR$^+$CD34$^+$CD45$^-$ bipotential hemoangiogenic progenitors derived in serum-free conditions

During embryogenesis, hematopoietic development is closely associated with endothelial lineage commitment [47,48], and

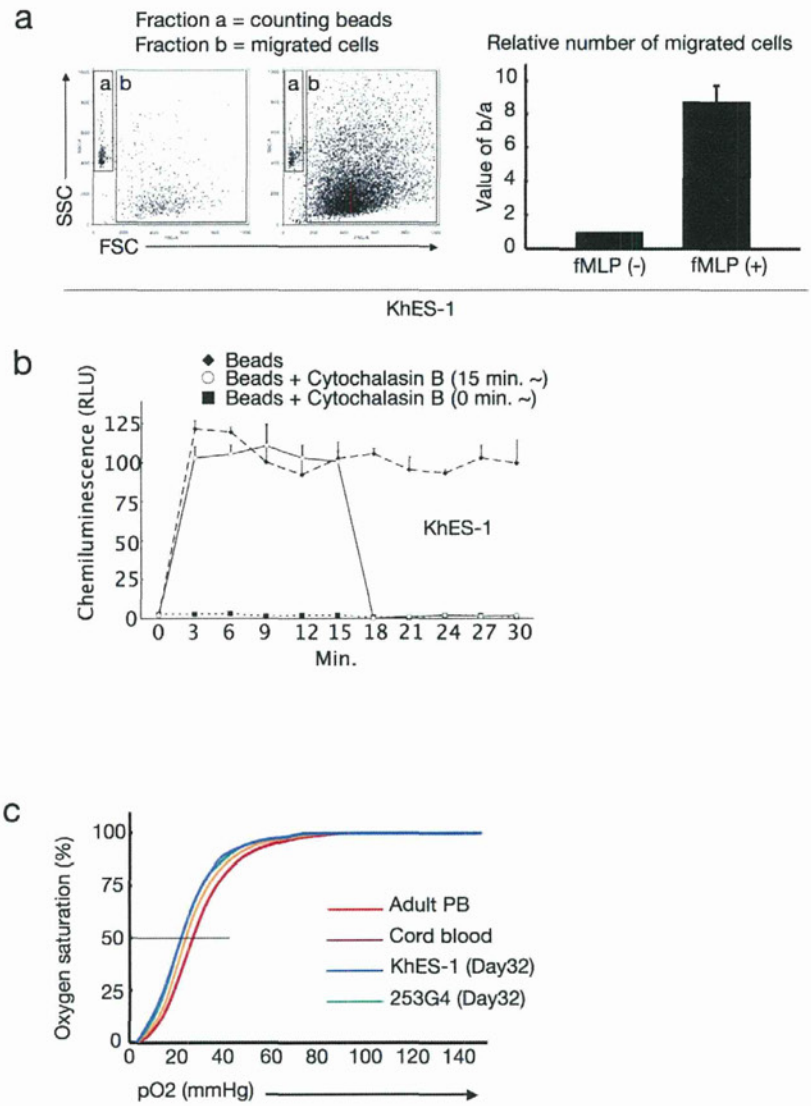

Figure 4. Functional blood cells derived from human ES/iPS cells. a. Number of migrated cells that permeated through the transwell membrane with or without fMLP. Values were normalised to the number of counting beads, and the control values were arbitrarily set to the condition without fMLP. Data from KhES-1 are shown as representative. **b.** Assay for phagocytosis-induced respiratory burst activity using chemiluminescent microspheres (luminol-binding microspheres). Abbreviation: RLU, relative light units. Data from KhES-1 are shown as representative. **c.** Oxygen dissociation curves of erythroid cells derived from human ES/iPS cells (harvested on day32 of differentiation), human cord blood, and adult peripheral blood. Where shown, bars represent standard deviation of the mean of three independent experiments.
doi:10.1371/journal.pone.0022261.g004

previous studies have demonstrated that ES cells can differentiate into the common multipotent progenitors that differentiate into both blood and endothelial cells at the single cell level on OP9 stroma [17,28,49]. Although the experiments described thus far demonstrated that the serum-free, xeno-cell-free culture condition supported human ES/iPS cell-derived hematopoiesis in an orderly manner, as observed during embryogenesis, it was unclear which day 6 fraction(s) developed into blood cells. To clarify this point, human ES cells stably expressing green fluorescent protein (GFP) were cultured, then 1×10^4 cells of $GFP^+KDR^-CD34^-CD45^-$ (Fraction A), $GFP^+KDR^+CD34^-CD45^-$ (Fraction B), and $GFP^+KDR^+CD34^+CD45^-$ (Fraction C) fractions were transferred on day 6 into a synchronous differentiation culture of unlabeled ES cells (Figure 6a). Nineteen days later (day 25 of differentiation), GFP^+ small round cell-containing colonies were observed predominantly in Fractions B and C, and FCM analysis of the entire culture confirmed the emergence of GFP^+CD45^+ cells mainly from Fraction C (Figure 6b). On the other hand, few blood cells positive for GFP were generated from Fraction A. These results were obtained with 2 independent strains of human ES cells (KhES1-EGFPneo on KhES-1 and KhES3-EGFPneo on KhES-3) (Figure 6c) and indicated that hematopoietic progenitors were present in the KDR^+ fraction, particularly in the KDR^+CD34^+ fraction, on day 6 of differentiation.

Finally, we performed a single-cell deposition assay by transferring single sorted human ES/iPS cell-derived $GFP^+KDR^+CD34^+CD45^-$ cells, which were negative for VE-cadherin, on day 6 into individual wells of 96-well plates coated

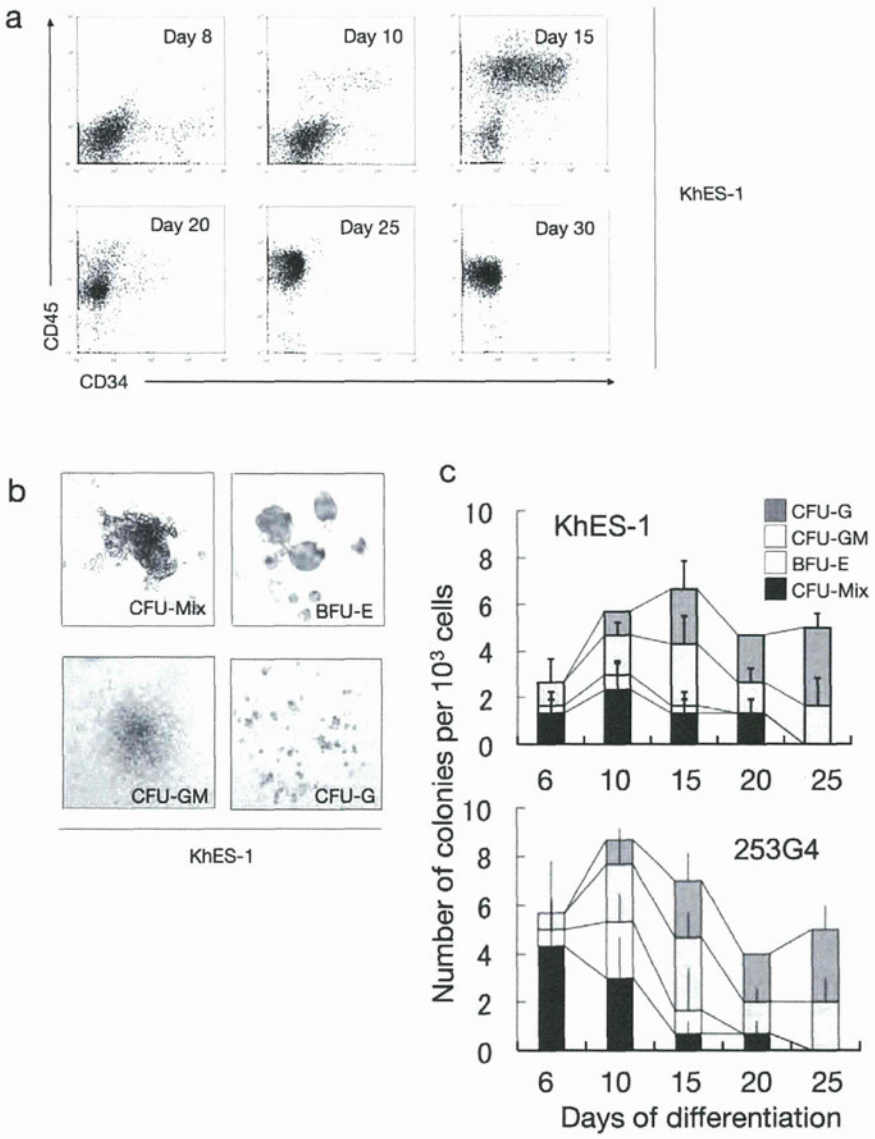

Figure 5. Hematopoietic stem/progenitor cells in culture. a. Sequential FCM analysis of cells harvested on indicated days showing the existence of $CD34^+CD45^+$ haematopoietic progenitor cells in culture. Data from KhES-1 are shown as representative. **b.** Various colony types on MTC-containing medium clonally emerged from single haematopoietic progenitor cells. Data from KhES-1 are shown as representative. **c.** Numbers of each colony type derived from different days of culture. Bars represent standard deviation of the mean of three independent experiments. Data from KhES-1 and 253G4 strains are shown as representative.
doi:10.1371/journal.pone.0022261.g005

with an OP9 cell layer. As shown in Figure 6d and e, the proportion of hematopoietic cell (HC) development, VE-cadherin$^+$ endothelial cell (EC) development, and HC plus EC development on day 20 were 9.0%, 6.8%, and 4.0%, respectively, for KhES-1 and 11.6%, 12.7%, and 8.3%, respectively, for 253G4 iPS cells. These results demonstrate that the common mesodermal progenitors that can differentiate into both blood and endothelial cells at the single-cell level are induced in our culture condition.

Discussion

In this study, we demonstrated the orderly mesodermal and hematopoietic differentiation of human ES and iPS cells in a novel serum-free monolayer culture condition. Simple manipulation of cytokine combinations facilitated robust, reproducible, and highly directed stepwise commitment to specific lineages of functional blood cells.

There are several reports on hematopoietic differentiation of human ES/iPS cells, such as murine-derived OP9 stromal cell coculture and feeder/serum-free EB formation systems [20,22,23,24,30,31,32,50]. However, two-dimensional cultures containing xeno-serum/cells often cause dependency on their lots, while complicated three-dimensional structures inside EBs make it difficult to assess and control conditions for inducing specific progenitors. Actually, few in vitro systems have been able to reliably reproduce hematopoietic development from mesodermal progenitors or model the in vivo coexistence of developing hematopoietic cells and their autologous microenvironments in

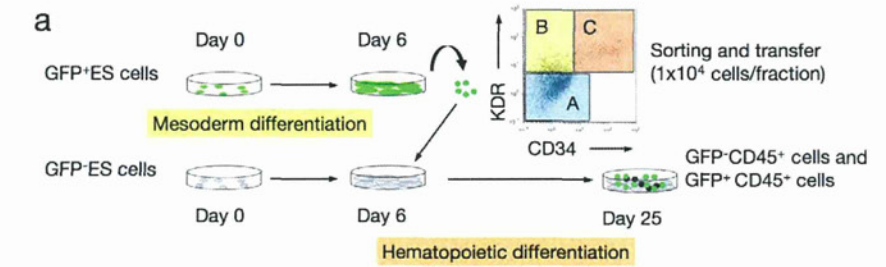

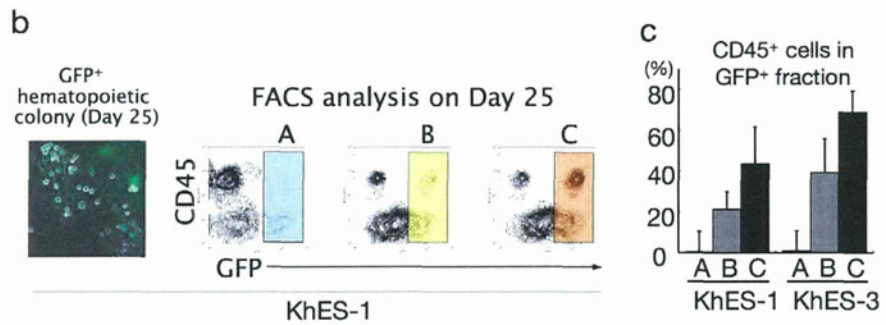

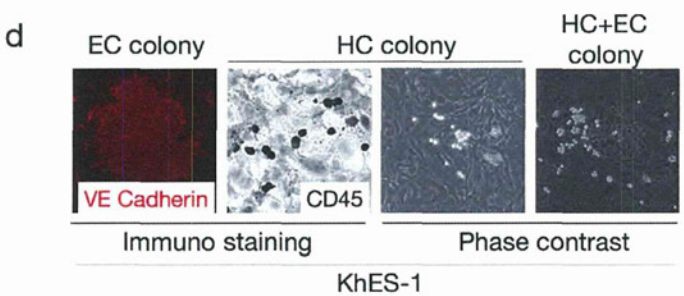

e

Clones	Only one cell 24 hours after sorting	At day 20		
		HC	EC	HC+EC
KhES-1 cells	176 wells	16 wells (9.0%)	12 wells (6.8%)	7 wells (4.0%)
256G4 iPS cells	181 wells	21 wells (11.6%)	23 wells (12.7%)	15 wells (8.3%)

HC : Haematopoietic colonies
EC : Endothelial colonies

Figure 6. Haematopoietic differentiation from KDR$^+$CD34$^+$ mesodermal progenitors. a. Schema of the protocol for measuring haematopoietic activities of depicted fractions on day 6. **b.** Each sorted fraction-derived haematopoiesis on day 25 detected by fluorescent microscopy and FCM analysis. Data from KhES-1 are shown as representative. **c.** Ratio of CD45$^+$ cells in GFP$^+$ fraction on day 25 showing the strongest haematopoietic activity of fraction C followed by fraction B. **d.** Single KDR$^+$CD34$^+$CD45$^-$ cell-derived haematopoietic colonies (HC), VE-cadherin$^+$ endothelial colonies (EC), and HC+EC colonies generated on OP9 cell layers. Data from KhES-1 are shown as representative. **e.** Number of wells that showed HC, EC, and EC+HC development.
doi:10.1371/journal.pone.0022261.g006

serum-free conditions. Our less labor-intensive and clearly defined monolayer culture facilitates observation of the stepwise development of pluripotent cells to blood cells via common hemoangiogenic progenitors and the behavior of hematopoietic cells on autologous stromal cells. Consequently, assays for elucidating differences in lineage specification of various ES/iPS cell strains, including hematopoietic potential, can be performed with high reproducibility. This is particularly important because individual pluripotent cell strains vary in differentiation potentials [51,52,53]. This study demonstrated quantitative differences in hematopoietic differentiation efficacy and lineage commitment among 4 ES/iPS cell strains.

Because human ES/iPS cells are feasible cell sources for various clinical applications, scientific and medical communities have shown continuing interest in hematopoietic stem cell induction from ES/iPS cells. Previous trials have indicated that murine ES cell-derived hematopoietic cells overexpressing HoxB4 [54] can replenish the bone marrow of lethally irradiated recipient mice. However, it remains a challenge to develop bona fide human hematopoietic stem cells with bone marrow reconstitution activity at the single-cell level. In our study, we observed many cobblestone area-forming cells, which reportedly indicate the existence of very immature hematopoietic progenitors. Moreover, FCM analyses and colony-forming assays suggested that ES and iPS human cell-

derived hematopoiesis in our method occurs through clonogenic hematopoietic stem/progenitor cells. We are in the process of determining in vivo repopulating ability of cells harvested from our culture by using serial transplantation into immunodeficient mice to assess the possibility of inducing feasible cell sources for various clinical applications, such as cell therapies and disease investigation.

Finally, time-lapse imaging strongly indicated crosstalk between hematopoietic cells and the autologous microenvironment composed of non-hematopoietic cells. Emerged blood cells move about actively and generate colonies in surrounding cell layers, suggesting the importance of a direct interaction between blood cells and microenvironmental cells for the maintenance, proliferation, and differentiation of stem or progenitor cells (Movie S3). In fact, a model of hematopoietic disorders triggered by mutation in the bone marrow microenvironment has been recently reported [55]. However, further investigation is necessary to identify the mechanisms responsible for such phenomena. Our culture may aid these investigations as it facilitates simple and sequential harvest of hematopoietic cells with minimal contamination by autologous adherent cell layers.

In conclusion, this study presents novel methods for analyzing the mechanisms of normal hematopoiesis in a robust, reproducible, and stepwise manner. Furthermore, employing gene-manipulated ES cells or disease-specific iPS cells will supply in vitro models of disease pathology, thereby providing further insights into hematological defects in conditions such as aplastic anemia and myelodysplastic syndromes.

Supporting Information

Movie S1 Time-lapse microscopic movie showing the morphological change in a single colony from day 0 to day 6 (initial differentiation). In this period, a colony begins forming a rosary-like morphology as it differentiates. The pictures were automatically taken every 8 minute by Biostation IM (Nikon Instruments, Tokyo, Japan).
(MOV)

Movie S2 Time-lapse microscopic movie showing the morphological change in a single colony from day 6 to day 25 (hematopoietic differentiation). After adding hematopoietic cytokines on day 6, hematopoietic cells first emerge from the areas near the edge of stratified zone. The pictures were automatically taken every 8 minute by Biostation IM (Nikon Instruments, Tokyo, Japan).
(MOV)

Movie S3 Close-up time-lapse microscopic movie showing hematopoietic cells moving about and generating colonies in surrounding cell layers. The pictures were automatically taken every 8 minute by Biostation IM (Nikon Instruments, Tokyo, Japan).
(MOV)

Acknowledgments

We are grateful to Kyowa Hakko Kirin Co. Ltd. for providing FP6. We thank N. Nakatsuji (Institute for Frontier Medical Sciences, Kyoto University) for providing human ES cells and S. Yamanaka (CiRA) for providing human iPS cells. We thank T. Tanaka (Nakahata-ken, CiRA) for his advice on undifferentiated human ES/iPS cell culture; T. Morishima (Graduate school of medicine, Kyoto University) for instructing the function assay of neutrophils; Y. Sasaki, S. Tomida, M. Yamane, and Y. Shima (Nakahata-ken, CiRA) for their excellent technical assistance; and H. Koyanagi (Nakahata-ken, CiRA), N. Hirakawa, Y. Ogihara, and G. Odani (Nikon Instruments Company) for their expertise in microscopic time-lapse monitoring. We thank H. Watanabe (Nakahata-ken, CiRA), M. Muraki, M. Terada, H. Konishi, C. Kaji, N. Takasu, and Y. Takao (Kenkyu-Senryaku-honbu, CiRA) for their superb administrative assistance.

Author Contributions

Conceived and designed the experiments: AN TH KU TN MKS. Performed the experiments: AN H. Sakai. Analyzed the data: AN TH KU KO IK H. Sakai. TN MKS. Contributed reagents/materials/analysis tools: H. Suemori H. Sakai. Wrote the manuscript: AN TN MKS.

References

1. Evans MJ, Kaufman MH (1981) Establishment in culture of pluripotential cells from mouse embryos. Nature 292: 154–156.
2. Thomson JA, Itskovitz-Eldor J, Shapiro SS, Waknitz MA, Swiergiel JJ, et al. (1998) Embryonic stem cell lines derived from human blastocysts. Science 282: 1145–1147.
3. Keller G (2005) Embryonic stem cell differentiation: emergence of a new era in biology and medicine. Genes Dev 19: 1129–1155.
4. Xu Y, Shi Y, Ding S (2008) A chemical approach to stem-cell biology and regenerative medicine. Nature 453: 338–344.
5. Shi Y, Do JT, Desponts C, Hahm HS, Scholer HR, et al. (2008) A combined chemical and genetic approach for the generation of induced pluripotent stem cells. Cell Stem Cell 2: 525–528.
6. Jaenisch R, Young R (2008) Stem cells, the molecular circuitry of pluripotency and nuclear reprogramming. Cell 132: 567–582.
7. Meissner A, Wernig M, Jaenisch R (2007) Direct reprogramming of genetically unmodified fibroblasts into pluripotent stem cells. Nat Biotechnol 25: 1177–1181.
8. Garcia-Porrero JA, Manaia A, Jimeno J, Lasky LL, Dieterlen-Lievre F, et al. (1998) Antigenic profiles of endothelial and hemopoietic lineages in murine intraembryonic hemogenic sites. Dev Comp Immunol 22: 303–319.
9. Choi K, Kennedy M, Kazarov A, Papadimitriou JC, Keller G (1998) A common precursor for hematopoietic and endothelial cells. Development 125: 725–732.
10. Wood HB, May G, Healy L, Enver T, Morriss-Kay GM (1997) CD34 expression patterns during early mouse development are related to modes of blood vessel formation and reveal additional sites of hematopoiesis. Blood 90: 2300–2311.
11. Shalaby F, Ho J, Stanford WL, Fischer KD, Schuh AC, et al. (1997) A requirement for Flk1 in primitive and definitive hematopoiesis and vasculogenesis. Cell 89: 981–990.
12. Sumi T, Tsuneyoshi N, Nakatsuji N, Suemori H (2008) Defining early lineage specification of human embryonic stem cells by the orchestrated balance of canonical Wnt/beta-catenin, Activin/Nodal and BMP signaling. Development 135: 2969–2979.
13. Flamme I, Breier G, Risau W (1995) Vascular endothelial growth factor (VEGF) and VEGF receptor 2 (flk-1) are expressed during vasculogenesis and vascular differentiation in the quail embryo. Dev Biol 169: 699–712.
14. Risau W (1995) Differentiation of endothelium. FASEB J 9: 926–933.
15. Risau W, Hallmann R, Albrecht U (1986) Differentiation-dependent expression of proteins in brain endothelium during development of the blood-brain barrier. Dev Biol 117: 537–545.
16. Huber TL, Kouskoff V, Fehling HJ, Palis J, Keller G (2004) Haemangioblast commitment is initiated in the primitive streak of the mouse embryo. Nature 432: 625–630.
17. Umeda K, Heike T, Yoshimoto M, Shiota M, Suemori H, et al. (2004) Development of primitive and definitive hematopoiesis from nonhuman primate embryonic stem cells in vitro. Development 131: 1869–1879.
18. Umeda K, Heike T, Yoshimoto M, Shinoda G, Shiota M, et al. (2006) Identification and characterization of hemoangiogenic progenitors during cynomolgus monkey embryonic stem cell differentiation. Stem Cells 24: 1348–1358.
19. Ji P, Jayapal SR, Lodish HF (2008) Enucleation of cultured mouse fetal erythroblasts requires Rac GTPases and mDia2. Nat Cell Biol 10: 314–321.
20. Vodyanik MA, Bork JA, Thomson JA, Slukvin II (2005) Human embryonic stem cell-derived CD34+ cells: efficient production in the coculture with OP9 stromal cells and analysis of lymphohematopoietic potential. Blood 105: 617–626.
21. Kitajima K, Tanaka M, Zheng J, Yen H, Sato A, et al. (2006) Redirecting differentiation of hematopoietic progenitors by a transcription factor, GATA-2. Blood 107: 1857–1863.
22. Takayama N, Nishikii H, Usui J, Tsukui H, Sawaguchi A, et al. (2008) Generation of functional platelets from human embryonic stem cells in vitro via ES-sacs, VEGF-promoted structures that concentrate hematopoietic progenitors. Blood 111: 5298–5306.

23. Choi KD, Vodyanik MA, Slukvin II (2009) Generation of mature human myelomonocytic cells through expansion and differentiation of pluripotent stem cell-derived lin-CD34+CD43+CD45+ progenitors. J Clin Invest 119: 2818–2829.
24. Choi KD, Yu J, Smuga-Otto K, Salvagiotto G, Rehrauer W, et al. (2009) Hematopoietic and endothelial differentiation of human induced pluripotent stem cells. Stem Cells 27: 559–567.
25. Niwa A, Umeda K, Chang H, Saito M, Okita K, et al. (2009) Orderly hematopoietic development of induced pluripotent stem cells via Flk-1(+) hemoangiogenic progenitors. J Cell Physiol 221: 367–377.
26. Timmermans F, Velghe I, Vanwalleghem L, De Smedt M, Van Coppernolle S, et al. (2009) Generation of T cells from human embryonic stem cell-derived hematopoietic zones. J Immunol 182: 6879–6888.
27. Morishima T, Watanabe K, Niwa A, Fujino H, Matsubara H, et al. (2011) Neutrophil differentiation from human-induced pluripotent stem cells. J Cell Physiol 226: 1283–1291.
28. Shinoda G, Umeda K, Heike T, Arai M, Niwa A, et al. (2007) alpha4-Integrin(+) endothelium derived from primate embryonic stem cells generates primitive and definitive hematopoietic cells. Blood 109: 2406–2415.
29. Ji J, Vijayaragavan K, Bosse M, Menendez P, Weisel K, et al. (2008) OP9 stroma augments survival of hematopoietic precursors and progenitors during hematopoietic differentiation from human embryonic stem cells. Stem Cells 26: 2485–2495.
30. Chadwick K, Wang L, Li L, Menendez P, Murdoch B, et al. (2003) Cytokines and BMP-4 promote hematopoietic differentiation of human embryonic stem cells. Blood 102: 906–915.
31. Wang L, Li L, Shojaei F, Levac K, Cerdan C, et al. (2004) Endothelial and hematopoietic cell fate of human embryonic stem cells originates from primitive endothelium with hemangioblastic properties. Immunity 21: 31–41.
32. Wang L, Menendez P, Shojaei F, Li L, Mazurier F, et al. (2005) Generation of hematopoietic repopulating cells from human embryonic stem cells independent of ectopic HOXB4 expression. J Exp Med 201: 1603–1614.
33. Nostro MC, Cheng X, Keller GM, Gadue P (2008) Wnt, activin, and BMP signaling regulate distinct stages in the developmental pathway from embryonic stem cells to blood. Cell Stem Cell 2: 60–71.
34. Gadue P, Huber TL, Paddison PJ, Keller GM (2006) Wnt and TGF-beta signaling are required for the induction of an in vitro model of primitive streak formation using embryonic stem cells. Proc Natl Acad Sci U S A 103: 16806–16811.
35. Kennedy M, D'Souza SL, Lynch-Kattman M, Schwantz S, Keller G (2007) Development of the hemangioblast defines the onset of hematopoiesis in human ES cell differentiation cultures. Blood 109: 2679–2687.
36. Martin R, Lahlil R, Damert A, Miquerol L, Nagy A, et al. (2004) SCL interacts with VEGF to suppress apoptosis at the onset of hematopoiesis. Development 131: 693–702.
37. Grigoriadis AE, Kennedy M, Bozec A, Brunton F, Stenbeck G, et al. (2010) Directed differentiation of hematopoietic precursors and functional osteoclasts from human ES and iPS cells. Blood 115: 2769–2776.
38. Takahashi K, Tanabe K, Ohnuki M, Narita M, Ichisaka T, et al. (2007) Induction of pluripotent stem cells from adult human fibroblasts by defined factors. Cell 131: 861–872.
39. Suemori H, Yasuchika K, Hasegawa K, Fujioka T, Tsuneyoshi N, et al. (2006) Efficient establishment of human embryonic stem cell lines and long-term maintenance with stable karyotype by enzymatic bulk passage. Biochem Biophys Res Commun 345: 926–932.
40. Suwabe N, Takahashi S, Nakano T, Yamamoto M (1998) GATA-1 regulates growth and differentiation of definitive erythroid lineage cells during in vitro ES cell differentiation. Blood 92: 4108–4118.
41. Nakahata T, Ogawa M (1982) Hemopoietic colony-forming cells in umbilical cord blood with extensive capability to generate mono- and multipotential hemopoietic progenitors. J Clin Invest 70: 1324–1328.
42. Nakahata T, Ogawa M (1982) Identification in culture of a class of hemopoietic colony-forming units with extensive capability to self-renew and generate multipotential hemopoietic colonies. Proc Natl Acad Sci U S A 79: 3843–3847.
43. Nakahata T, Spicer SS, Ogawa M (1982) Clonal origin of human erythro-eosinophilic colonies in culture. Blood 59: 857–864.
44. Uchida T, Kanno T, Hosaka S (1985) Direct measurement of phagosomal reactive oxygen by luminol-binding microspheres. J Immunol Methods 77: 55–61.
45. Ma F, Ebihara Y, Umeda K, Sakai H, Hanada S, et al. (2008) Generation of functional erythrocytes from human embryonic stem cell-derived definitive hematopoiesis. Proc Natl Acad Sci U S A 105: 13087–13092.
46. Fujimi A, Matsunaga T, Kobune M, Kawano Y, Nagaya T, et al. (2008) Ex vivo large-scale generation of human red blood cells from cord blood CD34+ cells by co-culturing with macrophages. Int J Hematol 87: 339–350.
47. Yamaguchi TP, Dumont DJ, Conlon RA, Breitman ML, Rossant J (1993) flk-1, an flt-related receptor tyrosine kinase is an early marker for endothelial cell precursors. Development 118: 489–498.
48. Asahara T, Murohara T, Sullivan A, Silver M, van der Zee R, et al. (1997) Isolation of putative progenitor endothelial cells for angiogenesis. Science 275: 964–967.
49. Kennedy M, Firpo M, Choi K, Wall C, Robertson S, et al. (1997) A common precursor for primitive erythropoiesis and definitive haematopoiesis. Nature 386: 488–493.
50. Grigoriadis AE, Kennedy M, Bozec A, Brunton F, Stenbeck G, et al. (2010) Directed differentiation of hematopoietic precursors and functional osteoclasts from human ES and iPS cells. Blood 115: 2769–2776.
51. Kim K, Doi A, Wen B, Ng K, Zhao R, et al. (2010) Epigenetic memory in induced pluripotent stem cells. Nature 467: 285–290.
52. Osafune K, Caron L, Borowiak M, Martinez RJ, Fitz-Gerald CS, et al. (2008) Marked differences in differentiation propensity among human embryonic stem cell lines. Nat Biotechnol 26: 313–315.
53. Ji H, Ehrlich LI, Seita J, Murakami P, Doi A, et al. (2010) Comprehensive methylome map of lineage commitment from haematopoietic progenitors. Nature 467: 338–342.
54. Kyba M, Perlingeiro RC, Daley GQ (2002) HoxB4 confers definitive lymphoid-myeloid engraftment potential on embryonic stem cell and yolk sac hematopoietic progenitors. Cell 109: 29–37.
55. Raaijmakers MH, Mukherjee S, Guo S, Zhang S, Kobayashi T, et al. (2010) Bone progenitor dysfunction induces myelodysplasia and secondary leukaemia. Nature 464: 852–857.

OPEN ACCESS Freely available online

PLoS one

Anti-Aβ Drug Screening Platform Using Human iPS Cell-Derived Neurons for the Treatment of Alzheimer's Disease

Naoki Yahata[1,2], Masashi Asai[2,3,4], Shiho Kitaoka[1,2], Kazutoshi Takahashi[1], Isao Asaka[1,2], Hiroyuki Hioki[2,5], Takeshi Kaneko[5], Kei Maruyama[3], Takaomi C. Saido[4], Tatsutoshi Nakahata[1], Takashi Asada[6], Shinya Yamanaka[1,7], Nobuhisa Iwata[2,4,8]*, Haruhisa Inoue[1,2,7]*

1 Center for iPS Cell Research and Application, Kyoto University, Kyoto, Japan, **2** Core Research for Evolutional Science and Technology, Japan Science and Technology Agency, Saitama, Japan, **3** Department of Pharmacology, Faculty of Medicine, Saitama Medical University, Saitama, Japan, **4** Laboratory for Proteolytic Neuroscience, RIKEN Brain Science Institute, Saitama, Japan, **5** Department of Morphological Brain Science, Graduate School of Medicine, Kyoto University, Kyoto, Japan, **6** Department of Neuropsychiatry, Institute of Clinical Medicine, University of Tsukuba, Tsukuba, Japan, **7** Yamanaka iPS Cell Special Project, Japan Science and Technology Agency, Saitama, Japan, **8** Graduate School of Biomedical Sciences, Nagasaki University, Nagasaki, Japan

Abstract

Background: Alzheimer's disease (AD) is a neurodegenerative disorder that causes progressive memory and cognitive decline during middle to late adult life. The AD brain is characterized by deposition of amyloid β peptide (Aβ), which is produced from amyloid precursor protein by β- and γ-secretase (presenilin complex)-mediated sequential cleavage. Induced pluripotent stem (iPS) cells potentially provide an opportunity to generate a human cell-based model of AD that would be crucial for drug discovery as well as for investigating mechanisms of the disease.

Methodology/Principal Findings: We differentiated human iPS (hiPS) cells into neuronal cells expressing the forebrain marker, Foxg1, and the neocortical markers, Cux1, Satb2, Ctip2, and Tbr1. The iPS cell-derived neuronal cells also expressed amyloid precursor protein, β-secretase, and γ-secretase components, and were capable of secreting Aβ into the conditioned media. Aβ production was inhibited by β-secretase inhibitor, γ-secretase inhibitor (GSI), and an NSAID; however, there were different susceptibilities to all three drugs between early and late differentiation stages. At the early differentiation stage, GSI treatment caused a fast increase at lower dose (Aβ surge) and drastic decline of Aβ production.

Conclusions/Significance: These results indicate that the hiPS cell-derived neuronal cells express functional β- and γ-secretases involved in Aβ production; however, anti-Aβ drug screening using these hiPS cell-derived neuronal cells requires sufficient neuronal differentiation.

Citation: Yahata N, Asai M, Kitaoka S, Takahashi K, Asaka I, et al. (2011) Anti-Aβ Drug Screening Platform Using Human iPS Cell-Derived Neurons for the Treatment of Alzheimer's Disease. PLoS ONE 6(9): e25788. doi:10.1371/journal.pone.0025788

Editor: Hitoshi Okazawa, Tokyo Medical and Dental University, Japan

Received May 26, 2011; **Accepted** September 10, 2011; **Published** September 30, 2011

Funding: This study was supported by Core Research for Evolutional Science and Technology, Japan Science and Technology Agency (HI & NI), and a research grant from the NOVARTIS Foundation for Gerontological Research (HI). The funders had no role in study design, data collection and analysis, decision to publish, or preparation of the manuscript.

Competing Interests: The authors have declared that no competing interests exist.

* E-mail: haruhisa@cira.kyoto-u.ac.jp (HI); iwata-n@nagasaki-u.ac.jp (NI)

Introduction

Alzheimer's disease (AD) is the most common cause of dementia in the elderly. It is characterized clinically by progressive declines in memory, executive function, and cognition. It is also characterized by pathological features, including the deposition of amyloid plaques and neurofibrillary tangles as well as neuronal and synaptic loss in particular areas of the brain [1]. Accumulation of amyloid β peptide (Aβ) is hypothesized to initiate the pathogenic cascade that eventually leads to AD. The amyloid hypothesis is based on an imbalance between the production and clearance of Aβ [2]. Aβ is produced by β- and γ-secretase-mediated sequential proteolysis of amyloid precursor protein (APP) and plays a central role in AD pathogenesis. Because β- and γ-secretases are directly involved in Aβ production, they are straightforward and attractive therapeutic targets for AD. A number of compounds that inhibit or modulate these secretase activities and Aβ levels *in vitro* and *in vivo* have to date been developed [3,4].

Development of a human, cell-based *in vitro* assay system is a basic requisite for drug discovery and for investigating mechanisms of the disease. Induced pluripotent stem (iPS) cells reprogrammed from somatic cells [5,6] provide an opportunity to easily generate and use patient-specific differentiated cells. Because previous AD assay systems using human cancer cell lines or primary rodent cell cultures did not perfectly present the human intracellular environment or components, human iPS (hiPS) cell-derived neuronal cells may enable the development of more efficient drugs, such as γ-secretase modulators, and the better elucidation of AD mechanisms. In this study, we successfully generated forebrain neurons from hiPS cells, and showed that Aβ production in

neuronal cells was detectable and inhibited by some typical secretase inhibitors and modulators. Thus, we provide a new platform for AD drug development, which might be applied to AD patient-specific iPS cell research.

Results

Differentiation of forebrain neurons from hiPS cells

Recently, forebrain neurons were successfully differentiated from mouse embryonic stem (ES) cells [7,8,9] and human ES and/or iPS cells [9,10,11]. The methods used for differentiation into spinal motor neurons and midbrain dopaminergic neurons required the morphogens retinoic acid (RA)/sonic hedgehog (SHH) and fibroblast growth factor 8 (FGF8)/SHH, respectively [11,12]. On the other hand, non-morphogens [10,11] or Lefty A and Dickkopf homolog 1 (Dkk1) [7,9] have been used for the induction of hiPS cells into forebrain neurons. Because amyloid plaques are observed in the cerebral cortex from the early stage of AD development [13], stem cells should be differentiated to at least forebrain neurons for *in vitro* assays in AD research.

We differentiated forebrain neurons from hiPS 253G4 cells, which were generated from human dermal fibroblasts using three reprogramming factors (Oct3/4, Sox2, and Klf4) [14], as described previously (Figure 1A) [12,15]. When neural stem cells were induced with Noggin and SB431542 for 17 days, we obtained cells that were positive for the neuroectodermal marker, Nestin (Figure 1B), as previously reported using human and monkey ES cells [15]. After culturing the cells with morphogen-free medium for days 17–24, Forkhead box G1 (Foxg1) expression was induced and Foxg1-positive cells were observed (Figure 1C, D) [11,15]. We also examined whether treatment with cyclopamine, an SHH inhibitor, increased the number of neurons presenting a glutamatergic phenotype as observed in mouse ES cells [8]. The expression level of vesicular glutamate transporter 1 (vGlut1), a glutamatergic marker, was not significantly increased by the addition of cyclopamine (final concentration 1 μM) from days 17 to 24 (data not shown). Therefore, we did not add cyclopamine in this period in subsequent experiments. At day 24, dissociated cells were reseeded on 24-well plates to further characterize the cells.

Next, we evaluated the hiPS cell-derived neuronal cells using four cortical layer-specific markers, T-brain-1 (Tbr1) and chicken ovalbumin upstream promoter transcription factor (COUP-TF)-interacting protein 2 (Ctip2) [9,10,11], and cut-like homeobox 1 (Cux1) and special AT-rich sequence-binding protein 2 (Satb2) [16]. Quantitative polymerase chain reaction (qPCR) revealed that expression levels of these markers were increased in a differentiation day-dependent manner (Figure 1E). At day 52, all four of these markers were visualized by immunocytochemistry (ICC) (Figure 1F). The percentages of marker-positive cells relative to the total number of cells were 62.2±2.9% for Tbr1, 11.9±3.0% for Ctip2, 82.6±5.0% for Cux1, and46.0±7.1% for Satb2. The population of each marker-positive cell was similar to that of data reported previously in human fetal brain around gestational week-20 [16]. In this experimental schedule, most cells expressed one or a few neocortical markers at day 52.

Characterization of hiPS cell-derived neuronal cells

Cells that were reseeded at day 24, were sparsely adhered to the culture plate and had proliferated and extended neurites in a time course-dependent manner as observed by the neuronal marker, class-III β-tubulin (Tuj1), and microtubule-associated protein 2 (MAP2) (Figure 2A). Tuj1 expression was almost saturated at day 45 (Figure 2B), but MAP2 and synapsin I expression were still increasing (Figure 2C, D). Synaptic development continued until day 52, and many synapsin I-positive puncta were detected by ICC at day 52 (Figure 2A). Expression of the glial marker, glial fibrillary acidic protein (GFAP), was highest at day 52 in this schedule (Figure 2E). This sequential expression pattern is similar to that reported recently in human pluripotent stem cell-derived neurons; the synapsin I-positive neuronal and GFAP-positive glial cultures at day 52 corresponded to the stage at which spontaneous neuronal activity was observed [17].

We then examined the neurotransmitter phenotypes of these differentiated neurons by evaluating the synthesizing enzymes for two typical cortical neurotransmitters, glutamate and γ-aminobutyric acid (GABA). Expression of the glutamatergic neuronal marker, phosphate-activated glutaminase (PAG) [18], and the GABAergic neuronal marker, glutamate decarboxylase (GAD), were observed by ICC at day 52 (Figure 2F). PAG- and GAD-positive neurons comprised 60±20% and 5±4% of total cells, respectively. Most of the Tuj1-positive neurons were also co-localized with the punctate signals of vGlut1 (Figure 2G). GABA-positive neurons comprised a similar population to the GAD-positive ones (Figure 2F, H). On the other hand, cholineacetyltransferase (ChAT) or vesicular acetylcholine transporter (VAChT)-positive cholinergic neurons were little observed at day 52, although their mRNA level increased with differentiation time (Figure S1). These data showed that a majority of differentiated neuronal cells possessed a glutamatergic phenotype in the present condition.

Differentiated neuronal cells express some components related to Aβ production

To evaluate their usefulness as an AD model, we measured the levels of Aβ secreted from the differentiated neuronal cells at days 38, 45, and 52. In the non-amyloidogenic pathway, α-secretase cleaves full-length APP (FL-APP) within the Aβ domain to the large soluble APP fragment (sAPPα) and APP-C terminal fragment α (CTFα) (Figure 3) [19]. In the amyloidogenic pathway, β-secretase, β-site APP cleaving enzyme 1 (BACE1), cleaves APP on the N-terminal side of the Aβ domain to soluble sAPPβ and APP-CTFβ (Figure 3). FL-APP and its cleavage products were increased in a time-course-dependent manner (Figure 3).

APP has three alternatively spliced isoforms: APP695, APP751, and APP770. APP695 is most abundantly expressed in neurons, whereas APP751 and APP770 show more ubiquitous expression patterns [20]. In cell lysates, we detected three separate APP variants on western blots. The estimated percentages of the neuron-dominant variant APP695 were 64.5±1.0%, 68.6±2.2%, and 69.6±2.1% at days 38, 45, and 52, respectively (Figures 3A and S2). The neuronal population at day 52 was approximately consistent with the sum of the percentages of the glutamatergic and GABAergic neurons mentioned above.

The aspartyl protease BACE1, the major β-secretase involved in cleaving APP, is a significant molecule for AD pathology because BACE1 protein levels and activity are increased in the brains of patients with the sporadic form of AD [21]. In our differentiated neurons, BACE1 protein levels were increased in a time course-dependent manner (Figure 4A, B), and we speculated that the upregulation of BACE1 protein levels may be due to a posttranscriptional mechanism [22]. BACE1 mRNA levels were slightly elevated with time (Figure 4B). These data may indicate that increased BACE1 protein levels were mainly induced by translational activation along with neuronal differentiation.

APP-CTFβ is cleaved to Aβ and APP intercellular domain (AICD) by γ-secretase (Figure 3). The γ-secretase complex consists of four core members, presenilin (PS; either PS1 or PS2), nicastrin, Pen-2, and Aph-1 [23]. PS1, nicastrin, and Pen-2 were detected by

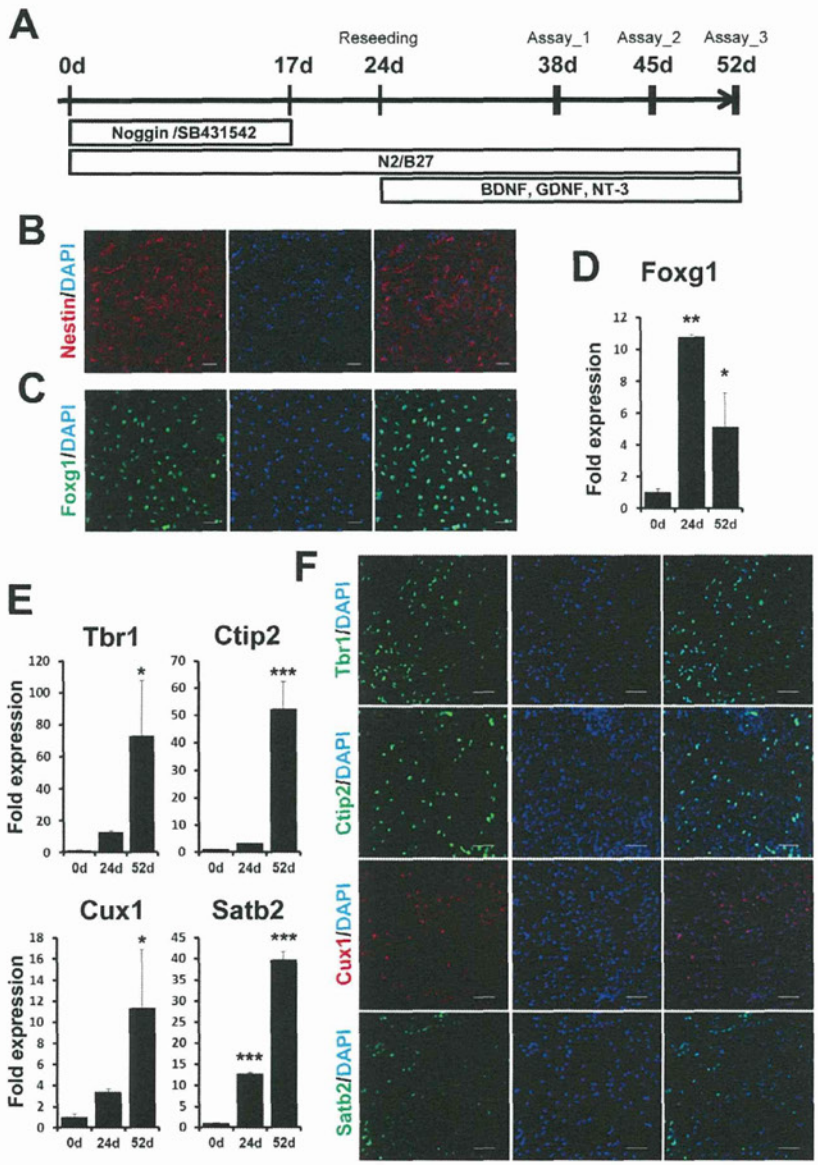

Figure 1. Differentiation of forebrain neurons from hiPS cells. (A) Experimental scheme of neural differentiation from hiPS cells, 253G4. Nestin-positive neuroepithelial cells (B) and Foxg1-positive cells (C) were observed at days 17 and 24, respectively. Scale bar, 50 μm. Expression levels of Foxg1 (D) and the neocortical markers Tbr1, Ctip2, Cux1, and Satb2 (E) at days 0, 24, and 52. Expression levels were measured by qPCR and normalized by that of GAPDH. "Fold expression" is shown as a ratio of day 24/day 0 or day52/day 0. Each column represents the mean ± SD of 3 assays. $^{*}p<0.05$, $^{**}p<0.01$, $^{***}p<0.001$, significantly different from day 0 by Dunnett's test. (F) ICC staining of Tbr1-, Ctip2-, Cux1- and Satb2-positive cells at day 52. Scale bar, 50 μm.
doi:10.1371/journal.pone.0025788.g001

western blotting, but their expression levels did not change markedly over time (Figure 4A, C). Aph-1 has two isoforms in human, Aph-1A and Aph-1B, which are considered to have different effects on the production of Aβ species related to AD [24]. Their expression levels measured by qPCR were relatively constant (Figure 4D). The Aph-1B/Aph-1A ratios also did not show significant differences among the time points analyzed here (Figure 4E).

Aβ has several species, including Aβ40 and Aβ42, which have emerged as two of the most robust Aβ measurements in brain. Recent studies suggest that Aβ40 and Aβ42 may have different effects on Aβ aggregation or oligomerization [25,26]. We measured Aβ40 and Aβ42 secreted into conditioned media for 2 days by sandwich ELISA. Both types of Aβ increased with time (Figure 5A). The level of Aβ40 was higher than that of Aβ42, compatible with previous reports [4,27,28,29,30]. Interestingly, the ratio of Aβ42/Aβ40 was highest at day 38, and there was no significant difference between days 45 and 52 (Figure 5B).

Inhibition of Aβ40 and Aβ42 secretion

We examined whether the differentiated neurons contained funtional β- and γ-secretases and whether Aβ secretion could be controlled. We selected the most effective, commercially available β- and γ-secretase inhibitors, β-secretase inhibitor IV (BSI) [31]

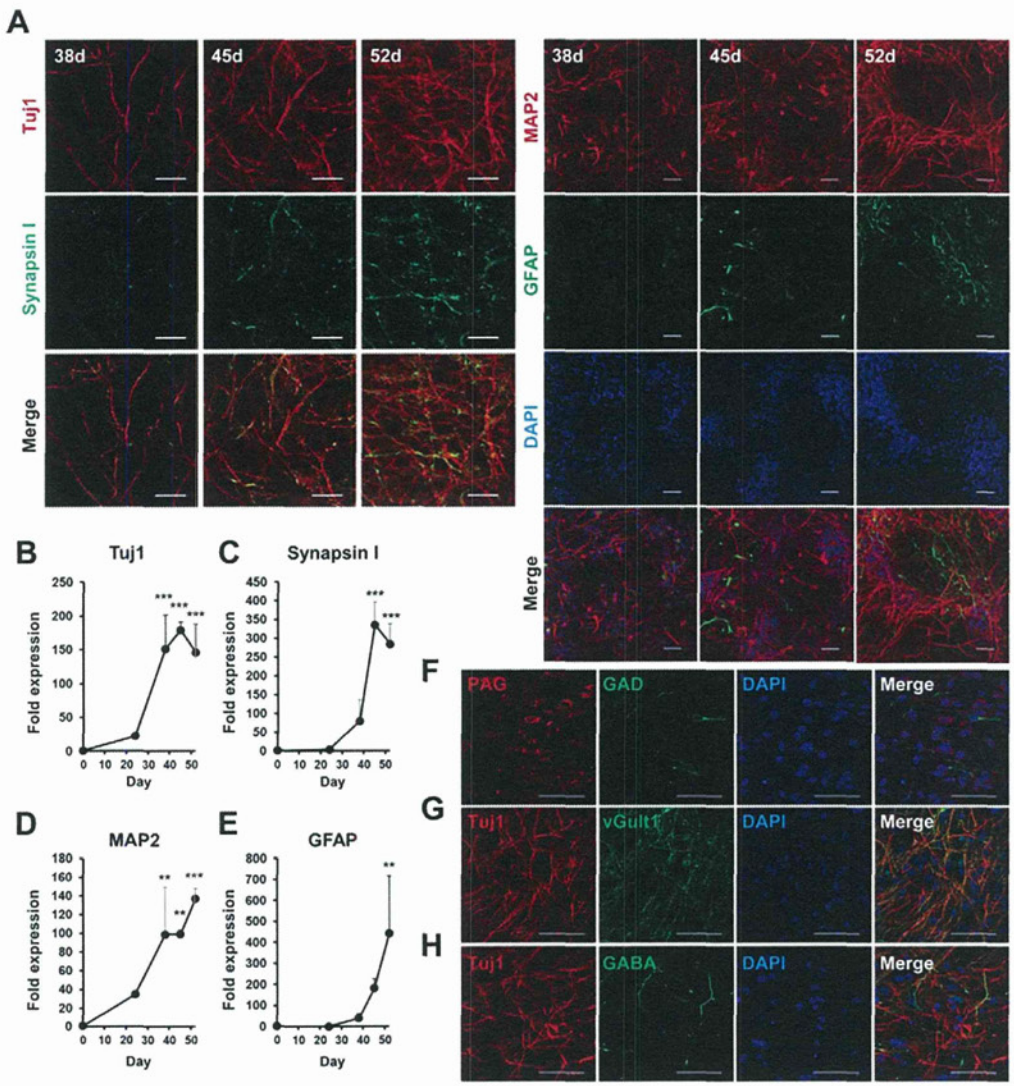

Figure 2. Characterization of neuronal and glial cells differentiated from hiPS cells. (A) Time-dependent morphological changes of cells reseeded in a 24-well plate. Neuronal and glial cells were stained by anti-Tuj1 (left; red), anti-synapsin I (left; green), anti-MAP2 (right; red), and anti-GFAP (right; green) antibodies and DAPI (right; blue) at 38, 45, and 52 days. Scale bar, left; 20 μm, right; 50 μm. Expression levels of Tuj1 (B), synapsin I (C), MAP2 (D), and GFAP (E) at days 0, 24, 38, 45, and 52 were measured by qPCR and normalized by that of GAPDH. "Fold expression" is the ratio of expression at each day compared to day 0. Each point represents mean ± SD of 3 assays. $^{*}p<0.05$, $^{**}p<0.01$, $^{***}p<0.001$, significantly different from day 0 by Dunnett's test. (F–H) Neurotransmitter phenotypes at day 52. PAG (red)- and GAD (green)-positive (F), vGlut1 (green)- and Tuj1 (red)-positive (G), and GABA (green)- and Tuj1 (red)-positive cells (H). Blue, DAPI. Scale bar, 50 μm.
doi:10.1371/journal.pone.0025788.g002

and γ-secretase inhibitor XXI/Compound E (GSI) [32], respectively. We also examined the effect of a non-steroidal anti-inflammatory drug (NSAID), sulindac sulfide [33], because some NSAIDs directly modulate γ-secretase activity to selectively lower Aβ42 levels [33,34]. The cells were treated with each drug for 2 days, and Aβ was monitored in the collected media at day 38 or 52.

There were different susceptibilities to all three drugs between days 38 and 52 (Figure 6) as revealed by two-way analysis of variance (ANOVA) [significant interaction between day and dose (BSI, $p<0.001$ in Aβ40 and Aβ42, respectively; GSI, $p<0.001$ in Aβ40 and Aβ42, respectively; NSAID, $p<0.001$ in Aβ42)]. Following BSI and NSAID treatment, secretion of Aβ40 and Aβ42 was decreased in a dose-dependent manner (Figure 6A, B, E, and F). NSAID especially showed more efficient inhibition of Aβ42 than that of Aβ40, consistent with a previous report [33]. Following GSI treatment (Figure 6C, D), secretion of both Aβ40 and Aβ42 was increased at lower doses (10^{-11}–10^{-8} M), but was inhibited at higher doses (10^{-7}–10^{-6} M) at day 52. This phenomenon, which is called a "gradual Aβ rise", was observed following the addition of other GSIs in a cell line system [35]. On the other hand, secretion of both Aβ40 and Aβ42 at day 38 showed a fast increase at lower doses (10^{-11}–10^{-9} M) (Aβ surge) and drastic decline at 10^{-8} M. We also examined the effects of these inhibitors on cell viability using the lactate dehydrogenase (LDH) assay. Two-day-treatments with the highest concentrations

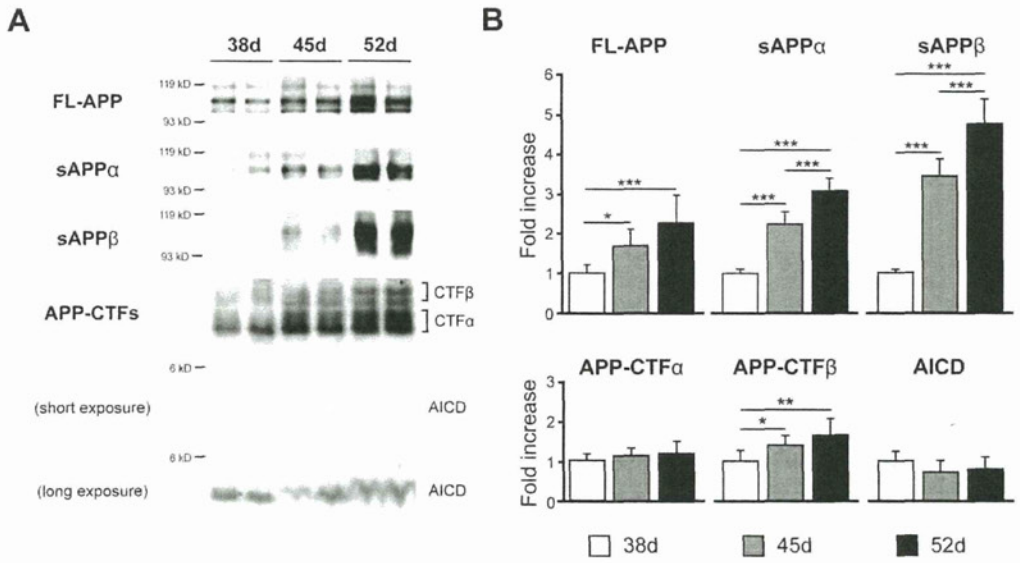

Figure 3. APP was expressed in hiPS cell-derived neuronal cells. HiPS cell-derived neuronal cells express full-length APP, sAPPα, sAPPβ, APP-CTFα, APP-CTFβ and AICD at 38, 45, and 52 days. (A) Representative western blots of APP and its fragments. (B) Each column represents mean ± SD of 8 samples measured by quantitative western blot analysis and normalized by that of β-actin. "Fold expression" represents the ratio of expression on the given day compared to day 38. $^{*}p<0.05$, $^{**}p<0.01$, $^{***}p<0.001$, Tukey's test.
doi:10.1371/journal.pone.0025788.g003

of BSI, GSI, or NSAID did not induce cell death (Table S1). We also traced these experiments using human ES (hES) cell (H9)-derived neuronal cells (Figure S4) because remaining expression of reprogramming factors, Oct3/4 and Klf4, were observed in hiPS cell (253G4)-derived neuronal cells (Figure S6). The Aβ production and its inhibition by these drugs in hES cell-derived neuronal cells were relatively similar to those in hiPS cell-derived ones (Figure S5). These data showed that BSI, GSI, and NSAID partially or fully blocked Aβ production in the hiPS cell-derived neuronal cells, indicating that these cells expressed functional β- and γ-secretases.

Discussion

AD is the most common cause of dementia in the elderly, with progressive neuronal loss in the cerebral cortex and hippocampal formation. Although the underlying etiology of most AD remains unclear, Aβ is thought to play a pivotal role in its pathogenesis. Studies from animal and cellular models have shown that mutations in the APP, PS1, and PS2 genes affected the production of Aβ, which contributes to the formation of amyloid plaques [19]. In several strains of mouse models, Aβ levels in brain tissue, cerebrospinal fluid (CSF), and plasma have been associated with AD pathogenesis and cognitive impairment [27,28,36]. Human samples from clinical AD patients have also been used for pathological and biochemical analyses to understand the etiology of AD. Aβ levels in CSF and plasma have been examined to evaluate their risks for AD [29,37], but brain tissues are only available postmortem for such analyses. On the other hand, immortalized human cell lines derived from kidney or brain, primary neurons derived from mice and rats, or cells artificially overexpressing APP or presenilin with or without familial AD mutations have been utilized for *in vitro* studies [4,30]. There is no doubt that these cells are quite different from living neurons in the human body in terms of innate qualities. Although we have had no choice until recently, important advances in technology of iPS cells may now provide the opportunity to use intact human-derived neuronal cells [38].

We evaluated whether iPS cell-derived neuronal cells could be applied to an *in vitro* cell-based assay system for AD research. In particular, further investigations into the metabolic mechanisms of Aβ are requisite for drug development to treat the brains of patients afflicted with AD. In this respect, we provide a profile of the molecular components associated with Aβ production in hiPS cell-derived neuronal cells and propose to add an Aβ assay system using these cells to the panel of generalized Aβ-monitoring systems (Table 1). Human neuronal cells are considered to provide more accurate human neuronal conditions within which to evaluate drug efficacy or toxicity than other human cell lines (e.g., cancer lines). Furthermore, we would be able to investigate how hiPS cell-derived neuronal cells reflect AD-related physiological and pathological conditions based on Aβ production.

In the present study, we characterized iPS cell-derived neuronal cells in terms of their expression of neuronal and glial markers by exposing them to Noggin and SB431542 during their differentiation (Figures 1 and 2). We observed increases in GFAP mRNA levels and in synapsin I-positive synaptic puncta at day 52. This was consistent with data showing that the existence of astrocytes promotes synaptic activity in human ES cell-derived neurons [40]. When differentiation occurred in the presence of non-morphogens, we obtained mainly glutamatergic neurons (Figure 2F, G), quite in line with previous reports of concerning hES and hiPS cells [10,11]. Expression of the forebrain marker Foxg1 suggests a default forebrain identity of the 253G4 iPS cells used in this study (Figure 1C, D). We also observed the expression of the neocortex-specific transcriptional factors Tbr1, Ctip2, Cux1, and Satb2 (Figure 1E, F). These expression schemes appear to mimic human neocortical development *in vitro* [16], although further analyses are needed to assist in understanding human neuronal subtype-specific differentiation.

This is the first study to observe the expression of APP, β- and γ-secretase, and the production of Aβ in hiPS cell-derived neuronal

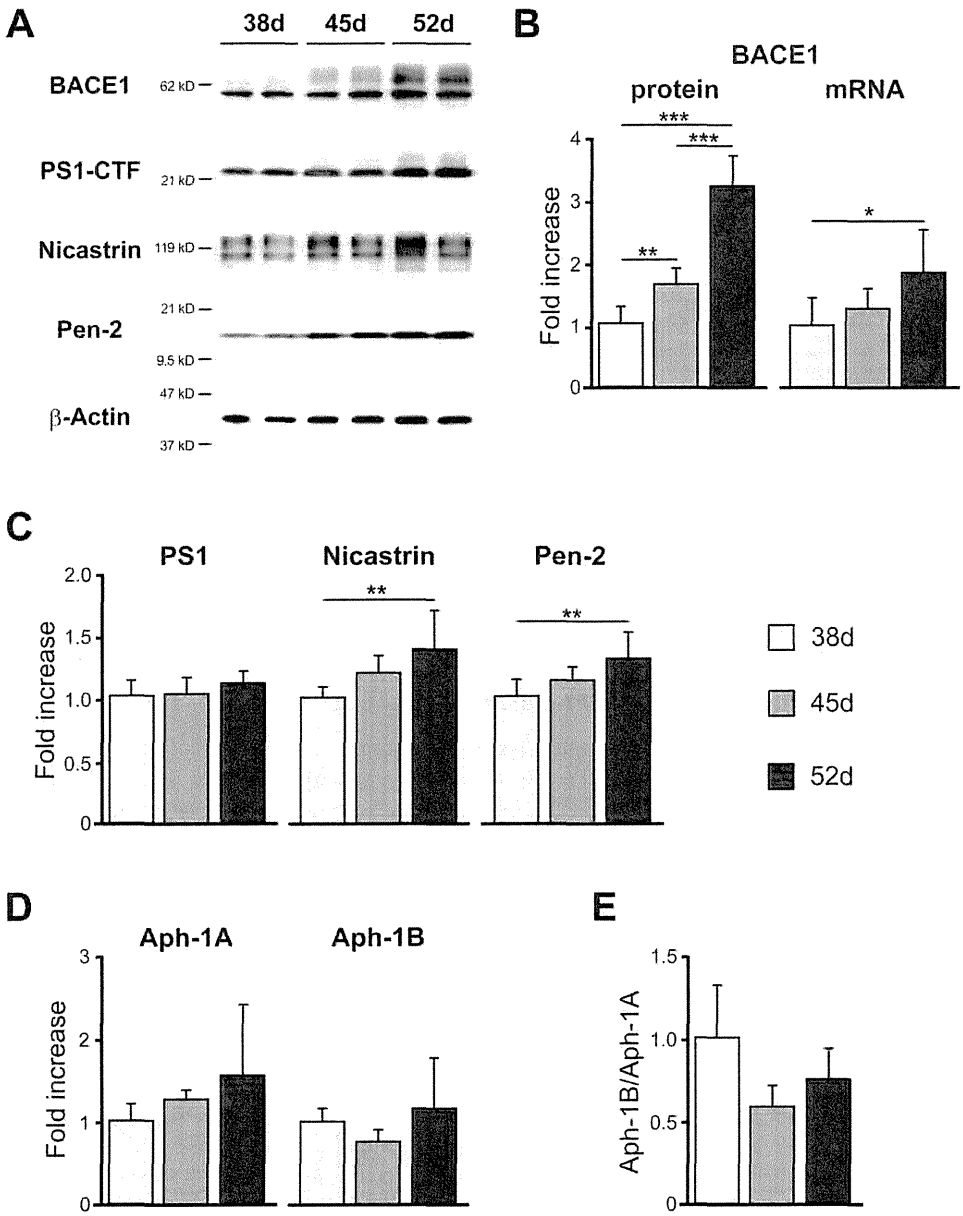

Figure 4. β-Secretase and γ-secretase components were expressed in hiPS cell-derived neuronal cells. The hiPS cell-derived neuronal cells express BACE1 protein and mRNA (B), γ-secretase components; presenilin 1(PS1), nicastrin, Pen-2 (C), and Aph-1A, and Aph-1B (D) at days 38, 45, and 52. Expression levels were quantified by western blot analysis (n = 8) (B, C) or qPCR (n = 3) (D) and normalized by that of β-actin. "Fold expression" represents the ratio of expression on the given day compared to day 38. (E) The ratio Aph-1B/Aph-1A. Data represent mean ± SD. (A) Representative western blots of BACE1 and γ-secretase components at 38, 45, and 52 days. $^{*}p<0.05$, $^{**}p<0.01$, $^{***}p<0.001$, Tukey's test.
doi:10.1371/journal.pone.0025788.g004

cells. APP, sAPPβ, APP-CTFβ and BACE1 protein levels were increased (Figures 3 and 4), but protein levels of γ-secretase components were not significantly different during the period from day 38 to 52 (Figure 4C, D). Aβ production in hiPS cell 253G4-derived neuronal cells increased with differentiation course (Figure 5A), however that in another hiPS cell 201B7 [5]- and in hES H9-derived neuronal cells did not increase (Figures S5 and S7) although all cell lines showed development of synapse (Figure S4A) as Aβ releasing site [41], indicating that besides synaptogenesis, subtle changes in localization and assembly of APP [42], BACE1, γ-secretase components would be critical for Aβ production.

The Aβ42/Aβ40 ratio unexpectedly showed a significant decrease from day 38 to 45 (Figure 5B). Serneels *et al.* reported that the γ-secretase complex containing Aph-1B was active and involved in the generation of amyloidogenic Aβ42 [24]. Our data showed that the Aph-1B/Aph-1A ratio did not change significantly with cell differentiation (Figure 4E); therefore, the Aβ42/Aβ40 ratio may be influenced by other unknown factors interacting directly or indirectly with γ-secretase.

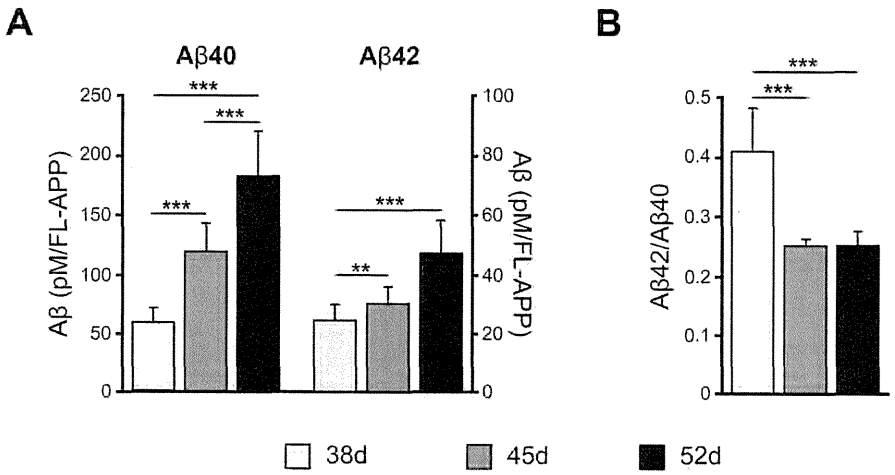

Figure 5. Aβ was produced in hiPS cell-derived neuronal cells. (A) Aβ40 or Aβ42 secreted into the conditioned media and FL-APP were measured by sandwich ELISA and western blot analysis, respectively. Expression level of Aβ was normalized by that of FL-APP. (B) Aβ42/Aβ40 ratios. Data represent the mean ± SD of 8 assays. $^{*,\#}p<0.05$, $^{**,\#\#}p<0.01$, $^{***,\#\#\#}p<0.001$, Tukey's test.
doi:10.1371/journal.pone.0025788.g005

BSI, GSI, and the NSAID sulindac sulfide inhibited Aβ production in this human neuronal cell system (Figure 6). The inhibitory effect on Aβ production by GSI showed a characteristic difference between days 38 (Aβ surge) and 52 (gradual Aβ rise) (Figure 6C, D). Aβ surge at day 38 was also observed in another hiPS cell (201B7)-derived neuronal cells (Figure S7) as well as in hES cell line, H9-derived ones (Figure S5). At day 38, GSI might promote neuronal differentiation with synaptogenesis via blocking Notch signaling [43] rather than inhibition of Aβ production, leading to Aβ surge. Another possible explanation for Aβ surge is that change in conformation or components of the γ-secretase affects the sensitivity of γ-secretase to GSI (total Aβ, Aβ40, Aβ42, and Aβ42/Aβ40), although levels of mRNA and the ration for Aph-1A and Aph-1B do not change between days 38 and 52 (Figure 4D, E) Thus, for precise Aβ monitoring in human stem cell-derived neuronal cells, it is necessary to use neuronal cells with a sufficient substrate level and synaptogenesis, because Aβ is released presynaptically, as mentioned above.

Some NSAIDs are known to preferentially lower Aβ42 [33,34]. Our data showed that sulindac sulfide was capable of inhibiting Aβ42 secretion at high concentrations ($\geq 10^{-5}$ M) (Figure 6F), although a few NSAIDs do not show therapeutic effects for AD. Negative results might be due to low γ-secretase modulator potency [44]. To discover novel effective drugs for modulating β- or γ-secretase activity, the *in vitro* hiPS cell-derived neuronal cell assay system might be expected to yield such drugs.

Familial AD patient specific neuronal cells generated by direct conversion (induced neuron, iN) show higher Aβ42/Aβ40 ratio than those of unaffected individuals [45]. Based on this report, hiPS/hES cell-derived neurons expressing mutant PS1, PS2, or APP may show higher Aβ42/Aβ40 ratio. Comparing to our results, the levels of Aβs in this assay (Aβ40; ~1.7 ng/ml at day 52) is higher than that using iN cells (Aβ40; ~0.1 ng/ml), although iN cells become functional neurons more quickly. The optimization of neuronal cell condition for comparison of the Aβ42/Aβ40 ratio between multiple iPS cell-derived neuronal cells may be required.

In conclusion, our findings indicate that hiPS cell-derived neuronal cells express functional β- and γ-secretases related to the production of Aβ in the present experimental conditions. In addition, our data provide the proof in principle that hiPS cell-derived neuronal cells can be applied to drug screening and AD patient-specific iPS cell research.

Materials and Methods

Antibodies and reagents

Primary antibodies used were as follows: mouse anti-Nestin (1:200, Millipore, Temecula, CA), mouse anti-Tuj1 (1:2000, Covance, Princeton, NJ), rabbit anti-GFAP (1:500, DAKO, Carpinteria, CA), rabbit anti-Synapsin I (1:500, Millipore), mouse anti-Cux1 (1:100, Abnova, Taipei, Taiwan), rabbit anti-Satb2 (1:1000, Abcam, Cambridge, UK), rat anti-Ctip2 (1:500, Abcam), rabbit anti-Tbr1 (1:500, Abcam), rabbit anti-vGlut1 (1:1000, Synaptic Systems, Göttingen, Germany), rabbit anti-Foxg1 (1:100, Abcam), rabbit anti-GABA (1:1000, Sigma-Aldrich, St. Louis, MO), rabbit anti-GAD65/67 (1:200, Millipore), mouse anti-PAG [46] (1:500), rabbit anti-APP (1:15000, Sigma-Aldrich), mouse anti-APP (1 μg/ml, Millipore), rabbit-anti BACE (1:2000, Merck, Darmstadt, Germany) mouse anti-PS1 loop C-terminus (1:1000, Millipore), rabbit anti-nicastrin (1 μg/ml, Thermo Scientific, Rockford, IL), rabbit anti-Pen-2 (1:1000, Invitrogen, San Diego, CA), mouse anti-MAP2 (1:200, Millipore), goat anti-ChAT (1:100, Millipore), guinea pig anti-VAChT (1:500, Millipore), and mouse anti-β-actin (1:15000, Sigma-Aldrich). We raised rabbit polyclonal antibodies against the carboxyl terminals of human sAPPα (hsAPPα) and sAPPβ using the KLH-conjugated synthetic peptides CRHDSGYEVHHQK and CKTEEISEVKM, respectively (Figure S3). All animal experiments were performed in compliance with the institutional guidelines at RIKEN Brain Science Institute, and were approved by the Animal Care and Use Committee (Permit number: H17-2B031). Each antibody was purified with a peptide-conjugated column [47]. Alexa Fluor 488 and Alexa Fluor 594-conjugated secondary antibodies (Invitrogen) were used for immunofluorescence.

The β-secretase inhibitor IV [31] and γ-secretase inhibitor XXI/Compound E [32] were purchased from Merck. Sulindac sulfide (NSAID) was purchased from Sigma-Aldrich.

Immunocytochemistry

Cells were fixed with 4% paraformaldehyde in phosphate buffered saline (PBS) for 30 min, and incubated in PBS

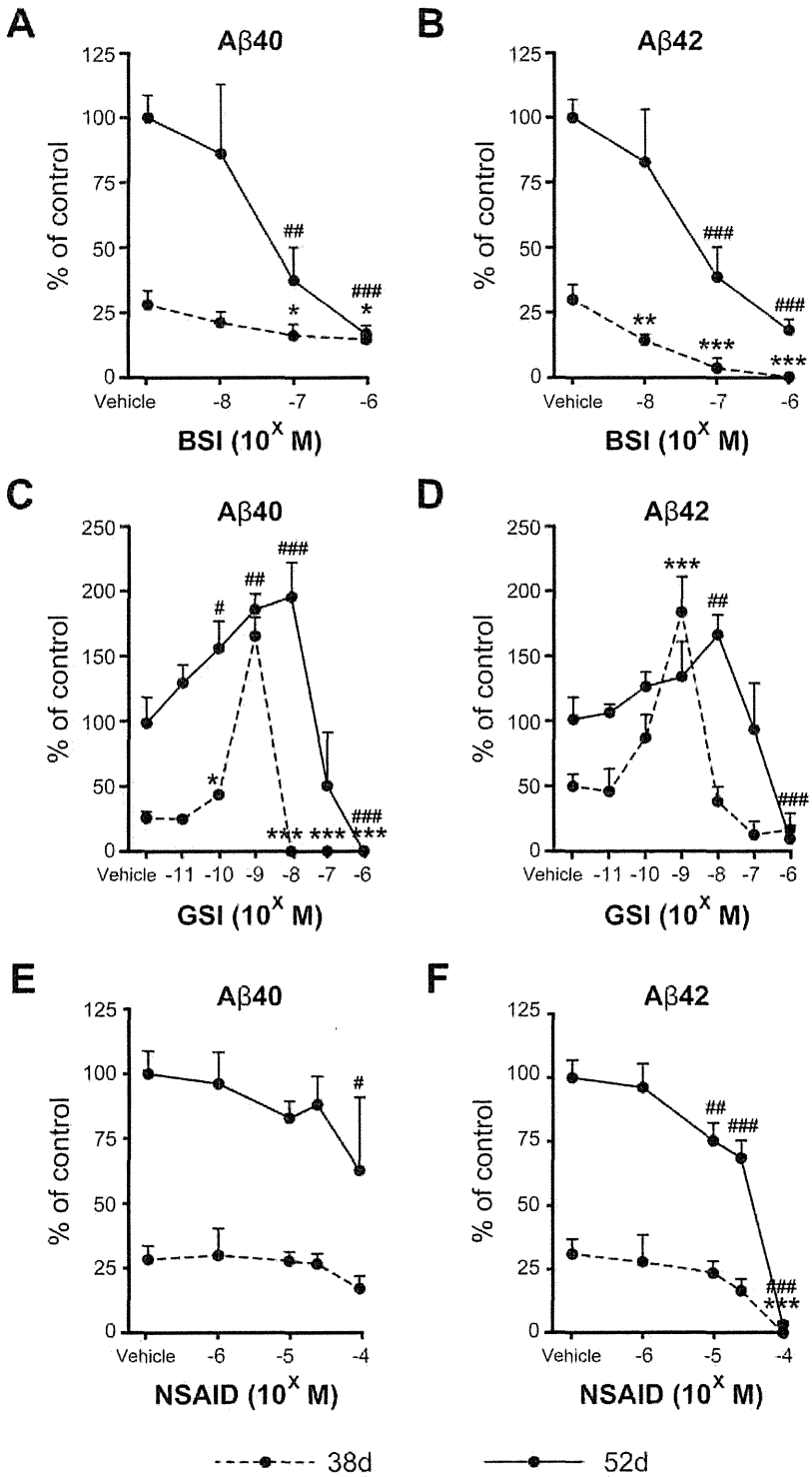

Figure 6. Aβ production was modulated by β- and γ-secretase inhibitors and an NSAID. β-Secretase inhibitor (BSI) (A, B), γ-secretase inhibitor (GSI) (C, D), and NSAID (E, F) were added into hiPS cell-derived neuronal cell cultures at day 36 (dotted line) and 50 (bold line), and two days later amounts of Aβ40 and Aβ42 secreted into the conditioned media were measured. The ratios Aβ40/FL-APP and Aβ42/FL-APP are expressed as percentages of the vehicle-treated group at day 52 and represent mean ± SD of 3 assays. A, B: There were significant main effects of day ($F(1, 16) = 72.5$ and 162.4, $p<0.001$ in Aβ40 and Aβ42, respectively) and dose ($F(3, 16) = 23.1$ and 45.7, $p<0.001$ in Aβ40 and Aβ42, respectively), and significant interaction between day and dose ($F(3, 16) = 13.0$ and 11.7, $p<0.001$ in Aβ40 and Aβ42, respectively) by 2-way ANOVA. C, D: There were significant main effects of day ($F(1, 28) = 240.5$ and 59.1, $p<0.001$ in Aβ40 and Aβ42, respectively) and dose ($F(6, 28) = 70.8$ and 37.8, $p<0.001$ in Aβ40 and Aβ42, respectively), and significant interaction between day and dose ($F(6, 28) = 23.5$ and 15.1, $p<0.001$ in Aβ40 and Aβ42, respectively) by